American Thoracic Society–European Respiratory Society Classification of the Idiopathic Interstitial Pneumonias: Advances in Knowledge since 2002[1]

Nicola Sverzellati, MD, PhD
David A. Lynch, MB
David M. Hansell, MD, FRCP, FRCR
Takeshi Johkoh, MD, PhD
Talmadge E. King, Jr, MD
William D. Travis, MD

In the updated American Thoracic Society–European Respiratory Society classification of the idiopathic interstitial pneumonias (IIPs), the major entities have been preserved and grouped into *(a)* "chronic fibrosing IIPs" (idiopathic pulmonary fibrosis and idiopathic nonspecific interstitial pneumonia), *(b)* "smoking-related IIPs" (respiratory bronchiolitis–associated interstitial lung disease and desquamative interstitial pneumonia), *(c)* "acute or subacute IIPs" (cryptogenic organizing pneumonia and acute interstitial pneumonia), and *(d)* "rare IIPs" (lymphoid interstitial pneumonia and idiopathic pleuroparenchymal fibroelastosis). Furthermore, it has been acknowledged that a final diagnosis is not always achievable, and the category "unclassifiable IIP" has been proposed. The diagnostic interpretation of the IIPs is often challenging because other diseases with a known etiology (most notably, connective tissue disease and hypersensitivity pneumonitis) may show similar morphologic patterns. Indeed, more emphasis has been given to the integration of clinical, computed tomographic (CT), and pathologic findings for multidisciplinary diagnosis. Typical CT-based morphologic patterns are associated with the IIPs, and radiologists play an important role in diagnosis and characterization. Optimal CT quality and a systematic approach are both pivotal for evaluation of IIP. Interobserver variation for the various patterns encountered in the IIPs is an issue. It is important for radiologists to understand the longitudinal behavior of IIPs at serial CT examinations, especially for providing a framework for cases that are unclassifiable or in which a histologic diagnosis cannot be obtained.

Abbreviations: H-E = hematoxylin-eosin, IIP = idiopathic interstitial pneumonia, IPF = idiopathic pulmonary fibrosis, NSIP = nonspecific interstitial pneumonia, RB-ILD = respiratory bronchiolitis–associated interstitial lung disease, UIP = usual interstitial pneumonia

RadioGraphics 2015; 35:1849–1872

Published online 10.1148/rg.2015140334

Content Codes: CH CT

[1]From the Section of Diagnostic Imaging, Department of Surgical Sciences, University of Parma, Via Gramsci 14, 43100 Parma, Italy (N.S.); Department of Radiology, National Jewish Health, Denver, Colo (D.A.L.); Department of Radiology, Royal Brompton Hospital, London, England (D.M.H.); Department of Radiology, Kinki Central Hospital of Mutual Aid Association of Public School Teachers, Hyogo, Japan (T.J.); Department of Medicine, University of California–San Francisco, San Francisco, Calif (T.E.K.); and Department of Pathology, Memorial Sloan Kettering Cancer Center, New York, NY (W.D.T.). Received December 9, 2014; revision requested January 22, 2015, and received February 12; accepted February 17. For this journal-based SA-CME activity, the authors D.A.L. and D.M.H. have provided disclosures (see p 1868); all other authors, the editor, and reviewers have disclosed no relevant relationships. **Address correspondence to** N.S. (e-mail: *nicola.sverzellati@unipr.it*).

See discussion on this article by McLoud (pp 1871–1872).

SA-CME LEARNING OBJECTIVES

After completing this journal-based SA-CME activity, participants will be able to:

■ Explain optimal-quality CT requirements for the evaluation of patients with IIP.

■ Distinguish fibrotic from nonfibrotic CT features of the IIPs.

■ Describe various longitudinal CT changes that may be seen in patients with any IIP.

See www.rsna.org/education/search/RG.

Introduction

The American Thoracic Society–European Respiratory Society classification of the idiopathic interstitial pneumonias (IIPs) underwent revision in 2013 (1). This update was not designed as a stand-alone document but as a supplement to the previous 2002 IIP classification, which defined key individual diseases and the best diagnostic approach to them (2). Pathologic patterns previously formed the basis for the classification of IIP subtypes, whereas in the update, more emphasis is given to the integration of clinical, computed tomographic (CT), and pathologic findings for multidisciplinary diagnosis (1).

TEACHING POINTS

- A systematic approach to CT of the chest in subjects suspected of having IIP entails the evaluation of image quality, the precise description of specific disease features with standard terminology, and the determination of the distribution of disease in the axial and craniocaudal planes. The most important next step is to determine whether the CT features permit a high-confidence diagnosis of UIP. In cases that do not meet strict criteria for UIP, the presence of traction bronchiectasis, architectural distortion, or volume loss usually permits distinction of fibrosing from nonfibrosing interstitial pneumonia.
- Terms such as *UIP pattern* and *NSIP pattern* are helpful in demonstrating that one is discussing the radiologic pattern rather than the associated clinical-pathologic syndrome. Indeed, it is important to appreciate that the CT patterns, especially those of the chronic fibrosing IIPs, may encompass several clinical-radiologic-pathologic entities; for example, NSIP and UIP patterns may be found in hypersensitivity pneumonitis and in association with connective tissue diseases.
- The primary role of CT is to separate chronic fibrosing lung diseases with a UIP pattern from those with non-UIP lesions, including those with findings associated with other IIPs (eg, RB-ILD, lymphoid interstitial pneumonia, and idiopathic pleuroparenchymal fibroelastosis).
- CT appearances of idiopathic pleuroparenchymal fibroelastosis are distinctive, with irregular pleural thickening and "tags" in the upper zones that merge with fibrotic changes in the subjacent lung, associated with evidence of substantial upper lobe volume loss (architectural distortion, traction bronchiectasis, and hilar elevation).
- The 2013 IIP consensus statement acknowledges, as did the 2002 consensus statement, that a final diagnosis is not always achievable.

In the updated classification, the major entities have been preserved and grouped into *(a)* "chronic fibrosing IIPs" (idiopathic pulmonary fibrosis [IPF] and idiopathic nonspecific interstitial pneumonia [NSIP]), *(b)* "smoking-related IIPs" (respiratory bronchiolitis–associated interstitial lung disease [RB-ILD] and desquamative interstitial pneumonia), and *(c)* "acute or subacute IIPs" (cryptogenic organizing pneumonia and acute interstitial pneumonia). In addition, idiopathic pleuroparenchymal fibroelastosis has been newly included and classified together with lymphoid interstitial pneumonia in a fourth group, "rare IIPs" (Table 1). In the updated classification, it has again been acknowledged that in a subset of cases, a final diagnosis cannot always be achieved despite extensive multidisciplinary discussion, and such cases are considered "unclassifiable" (1).

More emphasis has been placed on the differential diagnosis, which is often challenging because other diseases with known causes may show similar morphologic patterns to the IIPs at both histologic examination and CT. An important addition is a disease behavior classification, which provides a framework for management of cases that are unclassifiable or in which a histologic diagnosis cannot be obtained (Table 2) (1). Importantly, imaging will play an ever-increasing role in monitoring IIP and in refining the diagnosis of chronic fibrosing lung diseases as their disease behavior becomes evident.

The authors of the updated IIP classification document reviewed MEDLINE publications relevant to key imaging questions for the years 2001–2011. However, there was inadequate space in the document to address several important imaging-related issues, for example, the key CT principles for the evaluation of IIP, the fundamental CT features of each entity, and the longitudinal behavior of these features. The purpose of this review article is to expand the literature search through June 2014, concentrating on the CT aspects of IIP that were not covered in depth in the 2013 classification but are nevertheless important to radiologists tasked with tackling this difficult group of disorders. First, the principles of radiologic IIP assessment are reviewed. Then the four IIP groups are covered: *(a)* chronic fibrosing IIPs, *(b)* smoking-related IIPs, *(c)* acute or subacute IIPs, and *(d)* rare IIPs. Finally, the category of unclassifiable IIP is discussed.

Key Principles for Radiologic Assessment of IIP

CT is pivotal for the evaluation of IIP. Optimal-quality CT requires the use of thin-section (<2-mm) reconstruction and high-spatial-resolution reconstruction. Images should be obtained during a full inspiration to total lung capacity (3). Despite the risk of increasing the radiation dose delivered to patients, volumetric CT acquisition with multidetector CT is generally preferred to noncontiguous imaging (4). Importantly, volumetric CT acquisition and derived multiplanar reconstructions *(a)* allow improved characterization of patchy disease; *(b)* allow better delineation of disease extent; *(c)* simplify analysis of disease distribution (5); *(d)* allow identification of ancillary findings such as nodules or bronchiectasis; *(e)* facilitate differentiation between honeycombing and traction bronchiectasis, which may be crucial to diagnose the UIP pattern, as shown in Figures 1 and 2 (6); and *(f)* optimize follow-up CT matching for any comparative evaluation in subjects with chronic IIPs.

Unless contraindicated, CT scanning of the lungs should be performed with a reduced-dose technique. Several tools are available to reduce the radiation exposure, including automatic tube current modulation, optimization of tube potential, beam-shaping filters, and dynamic z-axis collimators (7,8). Acceptable CT images can be

Table 1: Radiologic Features and Differential Diagnosis of the IIPs

IIP Group and Clinical-Radiologic-Pathologic Diagnosis	CT Pattern	Typical CT Distribution	Typical CT Findings	CT Differential Diagnosis
Chronic fibrosing IIPs				
IPF	Usual interstitial pneumonia (UIP)	Peripheral, subpleural, basal	Reticular opacities, honeycombing, traction bronchiectasis or bronchiolectasis, architectural distortion, focal ground-glass attenuation	Collagen vascular disease, hypersensitivity pneumonitis, asbestosis, sarcoidosis
Idiopathic NSIP	NSIP	Peripheral, basal, symmetric	Ground-glass attenuation, irregular lines, traction bronchiectasis, consolidation	UIP, desquamative interstitial pneumonia, cryptogenic organizing pneumonia, hypersensitivity pneumonitis
Smoking-related IIPs				
Desquamative interstitial pneumonia	Desquamative interstitial pneumonia	Lower zone, peripheral predominance in most cases	Ground-glass attenuation, reticular lines, cysts	RB-ILD, NSIP, hypersensitivity pneumonitis
RB-ILD	Respiratory bronchiolitis	Often upper lung predominant, centrilobular	Bronchial wall thickening, centrilobular nodules, patchy ground-glass opacity	Desquamative interstitial pneumonia, NSIP, hypersensitivity pneumonitis
Acute or subacute IIPs				
Cryptogenic organizing pneumonia	Organizing pneumonia	Subpleural or peribronchial	Patchy consolidation or nodules, perilobular pattern, reverse halo sign	Infection, aspiration, eosinophilic pneumonia, NSIP, vasculitis, sarcoidosis, mucinous adenocarcinoma, lymphoma
Acute interstitial pneumonia	Diffuse alveolar damage	Diffuse or patchy	Consolidation and ground-glass opacity, often with lobular sparing; traction bronchiectasis later	Hydrostatic edema, pneumonia, pulmonary hemorrhage, acute eosinophilic pneumonia
Rare IIPs				
Lymphoid interstitial pneumonia	Lymphoid interstitial pneumonia	More commonly, lower lung predominant	Centrilobular nodules, ground-glass attenuation, septal and bronchovascular thickening, thin-walled cysts	NSIP, sarcoidosis, Langerhans cell histiocytosis and other cystic lung diseases
Idiopathic pleuroparenchymal fibroelastosis	Idiopathic pleuroparenchymal fibroelastosis	Peripheral, upper lung predominant	Pleural thickening and subpleural fibrotic changes	Sarcoidosis, pneumoconiosis, familial pulmonary fibrosis, connective tissue disease, hypersensitivity pneumonitis

obtained in all but the most obese patients by using a reference dose of 80 mAs. Although the use of a lower dose with standard reconstruction methods can adversely affect image interpretation or disease detection, extremely low mAs (eg, 30–40 mAs) may be used for follow-up CT (9) (Fig 3). However, noncontiguous CT scanning might be used in younger subjects or those in whom substantial changes (eg, disease regression) are expected. Because the definition of a "low-dose" study is still evolving, CT protocols for imaging IIP should be tailored for each individual by considering the principle of "as low as reasonably achievable" (ALARA) for the dose.

Prone CT is important if dependent opacification, mimicking disease, is depicted on supine images (10). Expiratory imaging is critical to identify airtrapping, which may be suggestive of an alternative diagnosis such as hypersensitivity pneumonitis or connective tissue disease (11) (Fig 4). Expiratory imaging may be performed with noncontiguous imaging and at a lower dose than inspiratory CT (12).

Systematic Approach to Chest CT

A systematic approach to CT of the chest in subjects suspected of having IIP entails the evaluation of image quality, the precise description of specific disease features with standard terminology (13), and the determination of the distribution of disease in the axial and craniocaudal planes. The most important next step is to determine whether the CT features permit a high-confidence diagnosis of UIP, as discussed in the following paragraphs. In cases that do not meet strict criteria for UIP, the presence of traction bronchiectasis, architectural distortion, or volume loss usually permits distinction of fibrosing from nonfibrosing interstitial pneumonia. In addition, the identification of ancillary features such as cysts, perilymphatic nodules, centrilobular nodules, mosaic attenuation, pleural thickening or effusions, a dilated esophagus, pleural plaques, sparing of the lung bases, or airtrapping may increase the suspicion of specific non-IIP entities (Table 3).

The terminology used in reporting radiologic findings on images should clearly indicate the differential diagnosis of the morphologic pattern, as well as the level of diagnostic confidence and the change in pattern or extent compared with previous images. Terms such as *UIP pattern* and *NSIP pattern* are helpful in demonstrating that one is discussing the radiologic pattern rather than the associated clinical-pathologic syndrome. Indeed, it is important to appreciate that the CT patterns, especially those of the chronic fibrosing IIPs, may encompass several clinical-radiologic-pathologic entities; for example, NSIP and UIP patterns may be found in hypersensitivity pneumonitis and in association with connective tissue diseases. Clinical information that may be important in refining the differential diagnosis may include the exposure history (including cigarette smoking), medications, and underlying connective tissue disease.

Table 2: Classification of IIP on the Basis of Disease Behavior

Reversible and self-limited disease (eg, many cases of RB-ILD)
Reversible disease with risk of progression (eg, cellular NSIP and some fibrotic NSIP, desquamative interstitial pneumonia, cryptogenic organizing pneumonia)
Stable with residual disease (eg, some fibrotic NSIP)
Progressive irreversible disease with potential for stabilization (eg, some fibrotic NSIP)
Progressive irreversible disease despite therapy (eg, IPF, some fibrotic NSIP)

An important aspect of the new classification system is the introduction of a new classification of IIP that is based on clinical observation of disease progression or regression (1). The categories included in this disease behavior classification are shown in Table 2. Although the role of routine follow-up CT studies in the screening of patients with IIP is not defined, CT in clinical practice may play a critical role in the serial observation of disease progression or improvement with time (eg, because no full functional assessment is available or for monitoring comorbidities) (Fig 5). In addition, the evaluation of the CT pattern (eg, nonfibrotic compared with fibrotic lung disease) may be combined with other clinical information (eg, the presence of a likely trigger, the short-term natural history, or the treated course) to predict disease progression; this may be particularly useful when surgical lung biopsy is not possible because of the disease severity or another contraindication. For example, an individual with predominant ground-glass abnormalities who is a heavy cigarette smoker is most likely to have slowly progressive or reversible lung disease.

As further emphasized in the updated classification document, radiologists should bear in mind that a key feature of the diagnostic approach is that it involves integrated and dynamic interactions among the clinician, the radiologist, and the histopathologist before a final diagnosis is rendered. In particular, the workup is regarded as a dynamic process whereby revision and refinement of the diagnosis may be necessary as new data or associations are identified (Fig 4, Table 4) (14).

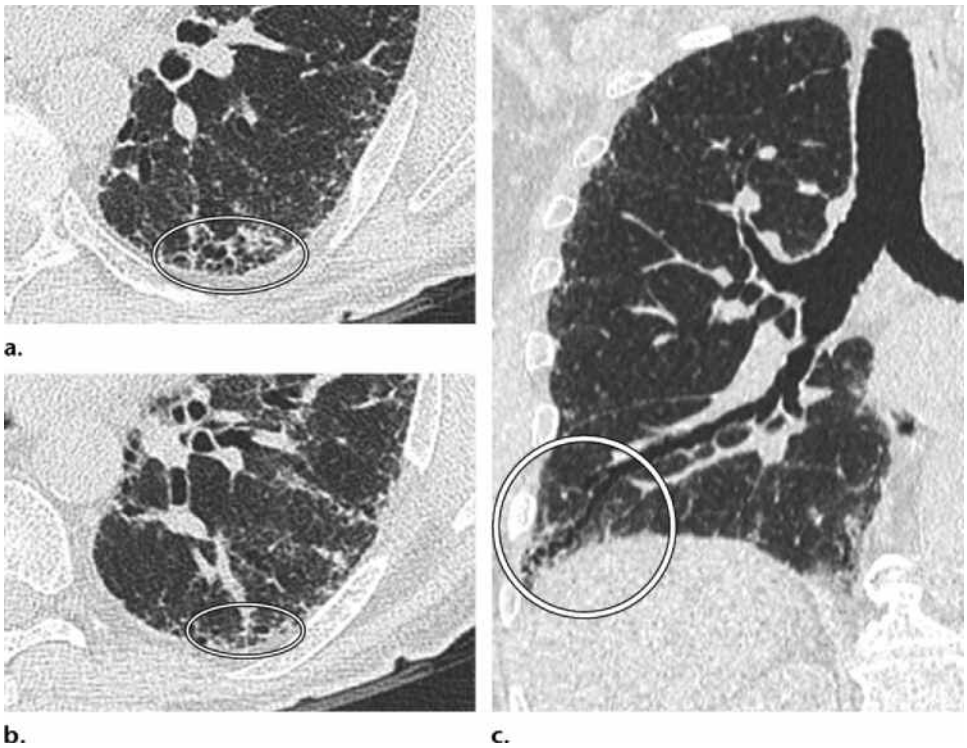

Figure 1. Diagnostic value of volumetric imaging. **(a, b)** Two axial thin-section CT images (**b** more caudal than **a**) obtained at a 10-mm interval were reconstructed from a volumetric CT acquisition and show subpleural reticular opacities admixed with cystic abnormalities (oval), resembling honeycombing. **(c)** Coronal reformatted CT image shows that those cystic abnormalities (circle) are peripheral traction bronchiectasis, a finding that improved the interpretation of these key CT abnormalities.

Figure 2. Diagnostic value of multiplanar imaging in idiopathic pleuroparenchymal fibroelastosis. Coronal reformatted CT image in a 66-year-old man shows the typical features of idiopathic pleuroparenchymal fibroelastosis, namely, bilateral irregular pleural thickening with a subjacent reticular pattern in the upper and mid zones (ovals). Also, coexisting reticular abnormalities are depicted with honeycombing in the lower lobes, findings that may represent associated UIP.

Figure 3. Reduced-dose CT imaging of interstitial lung disease. Axial CT image obtained with a reduced dose (30 mAs, 120 kVp, no dose modulation) in a 52-year-old man shows centrilobular fluffy nodules and peripheral ground-glass opacity admixed with mild paraseptal emphysema in a heavy smoker with a cough and a mild restrictive deficit at pulmonary function testing. The diagnosis is presumed RB-ILD.

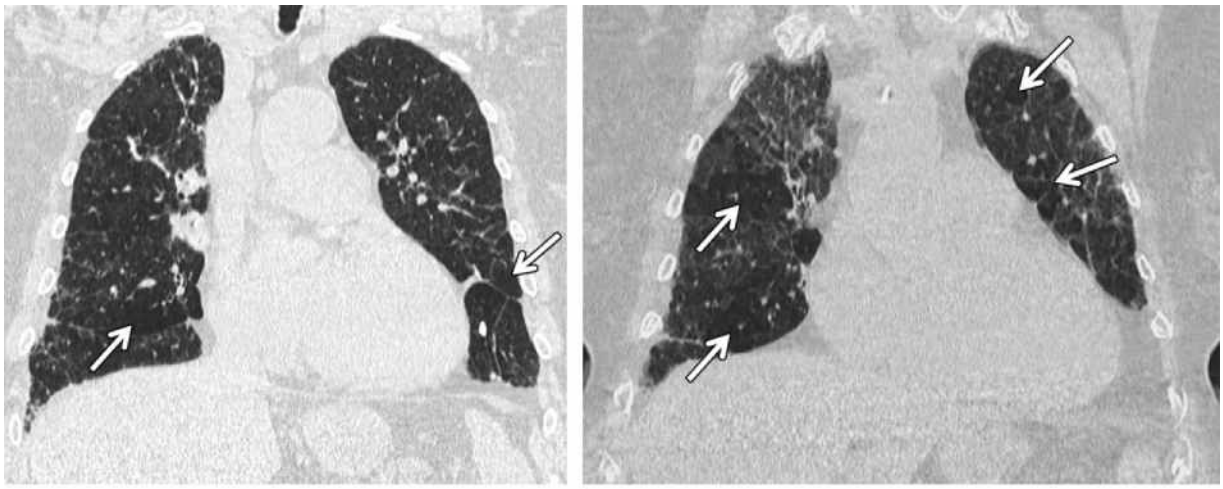

a. b.

Figure 4. Key ancillary CT findings for the multidisciplinary diagnosis of hypersensitivity pneumonitis in a 56-year-old woman with chronic hypersensitivity pneumonitis. **(a)** Coronal reformatted CT image obtained at suspended inspiration shows a reticular pattern with no particular zonal distribution and associated parenchymal distortion; areas of decreased attenuation (arrows) are also depicted. **(b)** Coronal expiratory CT image shows that the conspicuity and extent of the areas of decreased attenuation (arrows) are increased at expiratory CT, indicating small airways involvement, an almost invariable finding in hypersensitivity pneumonitis. CT findings led clinicians to reconsider the case and identify previously occult exposure to avian antigens.

Table 3: CT Findings That May Lead to Diagnosis of a Non-IIP Entity

Specific CT Finding	Non-IIP Entity
Cysts	Langerhans cell histiocytosis, lymphangioleiomyomatosis
Perilymphatic nodules	Sarcoidosis, chronic berylliosis, lymphangitic carcinomatosis, lymphoma
Centrilobular nodules	Hypersensitivity pneumonitis
Tree-in-bud pattern	Infection, aspiration, other forms of bronchiolitis
Mosaic attenuation or multilobular airtrapping	Hypersensitivity pneumonitis, obliterative bronchiolitis

Interobserver Variation

Variation occurs among observers for both the identification of individual CT signs of IIP, notably honeycombing (15), and for the subtypes of the IIPs (eg, UIP and NSIP). The interobserver agreement for the CT diagnosis of UIP/IPF is moderate to excellent (16–18). NSIP accounts for the majority of disagreements among observers for the IIPs, particularly the distinction of NSIP from UIP, desquamative interstitial pneumonia, and, less frequently, organizing pneumonia (19–21). Interobserver variation may be problematic even among experienced radiologists, particularly in those difficult cases that are commonly referred for surgical biopsy (20). However, as might be expected, interobserver agreement is greater among academic radiologists than among community radiologists (22).

The level of interobserver agreement for the assessment of individual CT signs in the IIPs is variable (16,23,24). In particular, interobserver agreement for honeycombing depends on the prevalence of other features, such as emphysema, that may mimic honeycombing (24,25). Given the critical importance of establishing the presence of honeycombing—the key diagnostic feature for establishing a CT diagnosis of UIP—this limitation needs to be appreciated.

In a multicenter study comprising a large IPF study population, agreement with regard to the presence or absence of honeycombing was recorded in 71.7% of cases between two core panel radiologists and was also similar to that reported for study-site radiologists (23). Likewise, in another large study, there was disagreement in approximately one-third of cases for the identification of honeycombing, particularly when this feature was mixed with traction bronchiectasis, large cysts, and superimposed paraseptal or centrilobular emphysema (15). Conversely, moderate interobserver agreement has been reported for the presence or absence of the CT sign

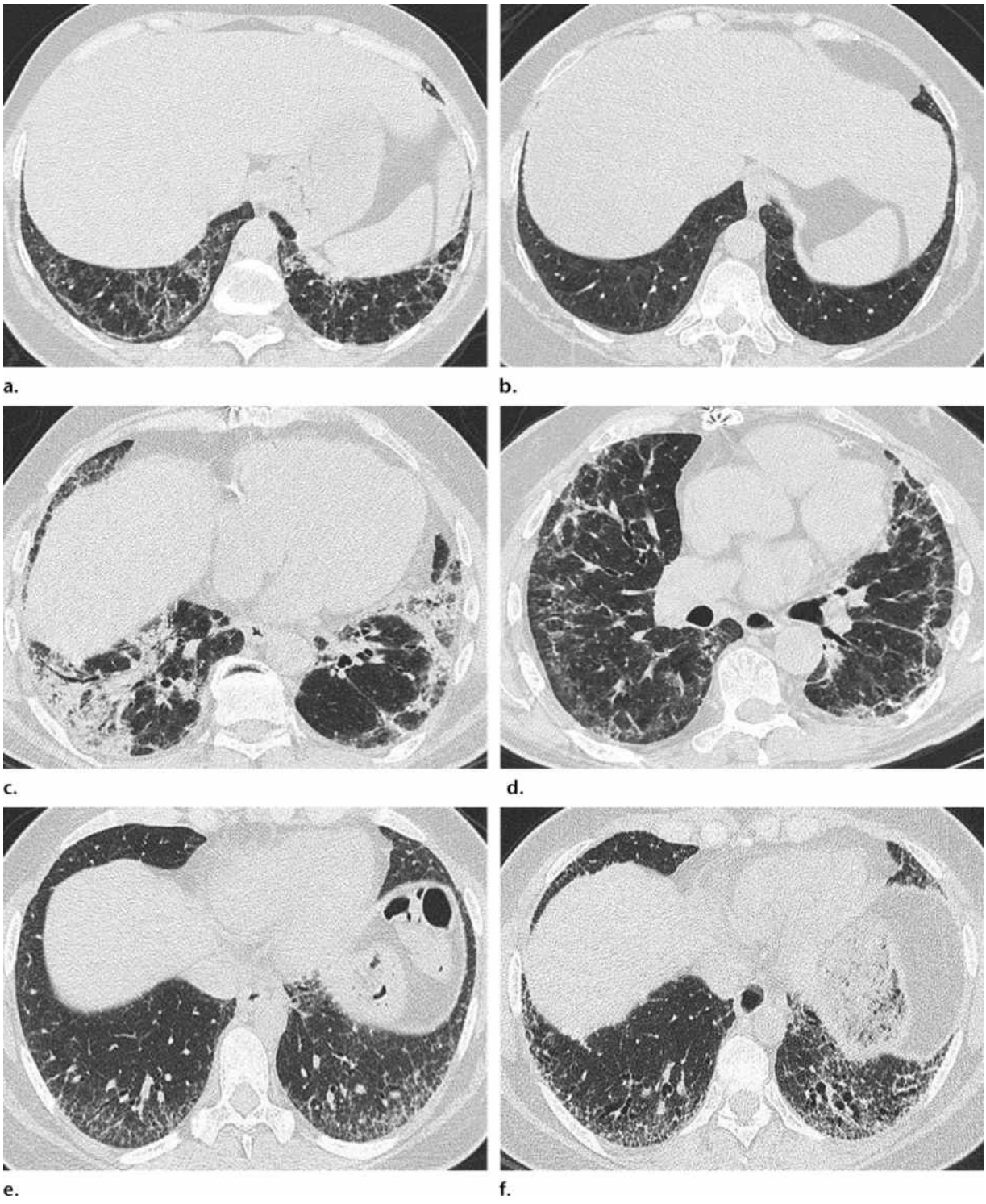

Figure 5. Examples of cases with a radiologic NSIP pattern that were classified according to disease behavior. **(a, b)** Axial CT image **(a)** of reversible and self-limited disease in a 40-year-old man with a cough and mild dyspnea shows a radiologic NSIP pattern characterized by reticular opacities sparing the subpleural regions of the lung and without obvious traction bronchiectasis; the axial follow-up CT image **(b)** obtained after steroid treatment shows resolution of the reticular abnormalities and residual mild ground-glass opacity. **(c, d)** Axial CT image **(c)** of reversible disease with the risk of progression in a 47-year-old woman shows a mixed NSIP and organizing pneumonia pattern of unknown cause; the axial short-term follow-up CT image **(d)** obtained after steroid treatment shows resolution of the consolidation, with a residual NSIP pattern characterized by peripheral reticular abnormality with subpleural sparing. One year later, this patient developed serologic evidence of antisynthetase syndrome. **(e, f)** Axial CT image **(e)** of progressive irreversible disease with the potential for stabilization in a 51-year-old woman with a lower lobe–predominant peripheral reticular abnormality and mild traction bronchiectasis, a "possible UIP pattern"; despite this, this patient refused to undergo surgical lung biopsy, and the axial follow-up CT image **(f)** showed that the reticular opacities and traction bronchiectasis increased after 6 months. Surgical lung biopsy was then performed, and the histologic findings showed an NSIP pattern that was stabilized by increasing the treatment with anti-inflammatory agents.

Table 4: Clinical and CT Features Suggestive That Histopathologic NSIP Pattern Does Not Indicate Idiopathic NSIP

Combined Clinical Features	CT Features	More Likely Multidisciplinary Diagnosis
Older age (>70 years), male sex, former or current smoker	Marked honeycombing	UIP/IPF
Younger age, critical exposures, nonsmoker, midinspiratory squeaks, lymphocytosis at examination of bronchoalveolar lavage fluid	Centrilobular nodules, airtrapping, relative sparing of lung bases	Hypersensitivity pneumonitis
Younger age, female sex, Raynaud syndrome, skin findings, musculoskeletal findings, positive serologic tests	Pleural effusion and pleural thickening, pericardial effusion, esophageal dilatation, disproportionate pulmonary arterial enlargement, airtrapping and abnormalities of airways away from lung fibrosis	Connective tissue disease, vasculitis
Younger age, multisystem involvement	Perilymphatic nodules in addition to reticulation	Fibrosing sarcoidosis

of traction bronchiectasis (16,26,27). Steps that can be taken to reduce interobserver variation in the diagnosis of IIPs would include adherence to standard descriptive terminology (13) and a reliance on standardized criteria (1,28).

Chronic Fibrosing IIPs

Idiopathic Pulmonary Fibrosis

IPF is defined as a specific form of chronic progressive fibrosing interstitial pneumonia of unknown cause that occurs primarily in older adults and is associated with the histopathologic or radiologic pattern of UIP. Prognosis is poor, with a median survival of less than 5 years (29). The diagnosis of IPF requires *(a)* exclusion of other known causes of interstitial lung disease, *(b)* the presence of a UIP pattern on CT images in patients not subjected to surgical lung biopsy, and *(c)* specific combinations of CT and surgical lung biopsy patterns in patients subjected to surgical lung biopsy. Indeed, multidisciplinary discussion forms the basis of the diagnostic algorithm and schema for correlating clinical, histologic, and radiologic findings in patients suspected of having IPF (28).

CT Features.—The role of CT in the diagnosis of IPF has been clearly defined in the latest IPF classification (28). In the appropriate clinical setting, the presence of a classic UIP pattern at CT is sufficient for the diagnosis of IPF, without the need for surgical lung biopsy. The characteristic CT features of UIP are a reticular pattern with honeycombing, often associated with traction bronchiectasis; ground-glass opacity may be depicted but is less extensive than the reticular abnormality (Table 1, Fig 6) (28). Such abnormalities are characteristically found in basal and peripheral areas, although the distribution is often patchy. The distribution may be asymmetric in as many as 25% of cases (30).

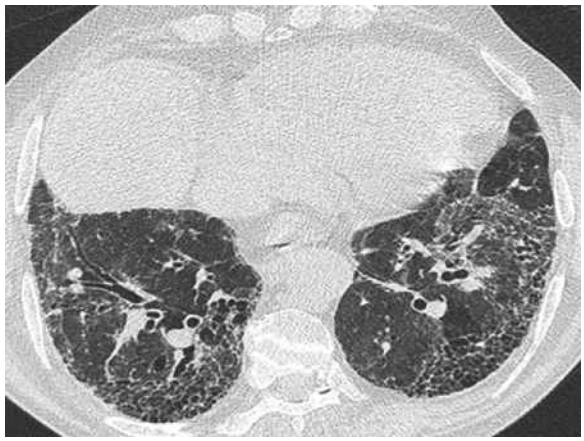

Figure 6. Fibrotic lung disease classified according to the IPF guidelines as the definite UIP pattern. Axial CT image in a 77-year-old man shows subpleural basal honeycombing with traction bronchiectasis, as well as reticular and ground-glass opacities. When idiopathic, this CT pattern is sufficient for the diagnosis of IPF.

A confident CT diagnosis of UIP is not usually made unless honeycombing is depicted. If honeycombing is absent but the imaging features otherwise meet the criteria for UIP (especially when the pattern is characterized by reticular opacities in a predominantly peripheral and basal distribution), the imaging features have been regarded as representing possible UIP, and surgical lung biopsy is necessary to make a definitive diagnosis (Fig 7) (28). However, in the findings from several recent studies, investigators have suggested that subjects with typical clinical features and CT appearances of UIP, but without

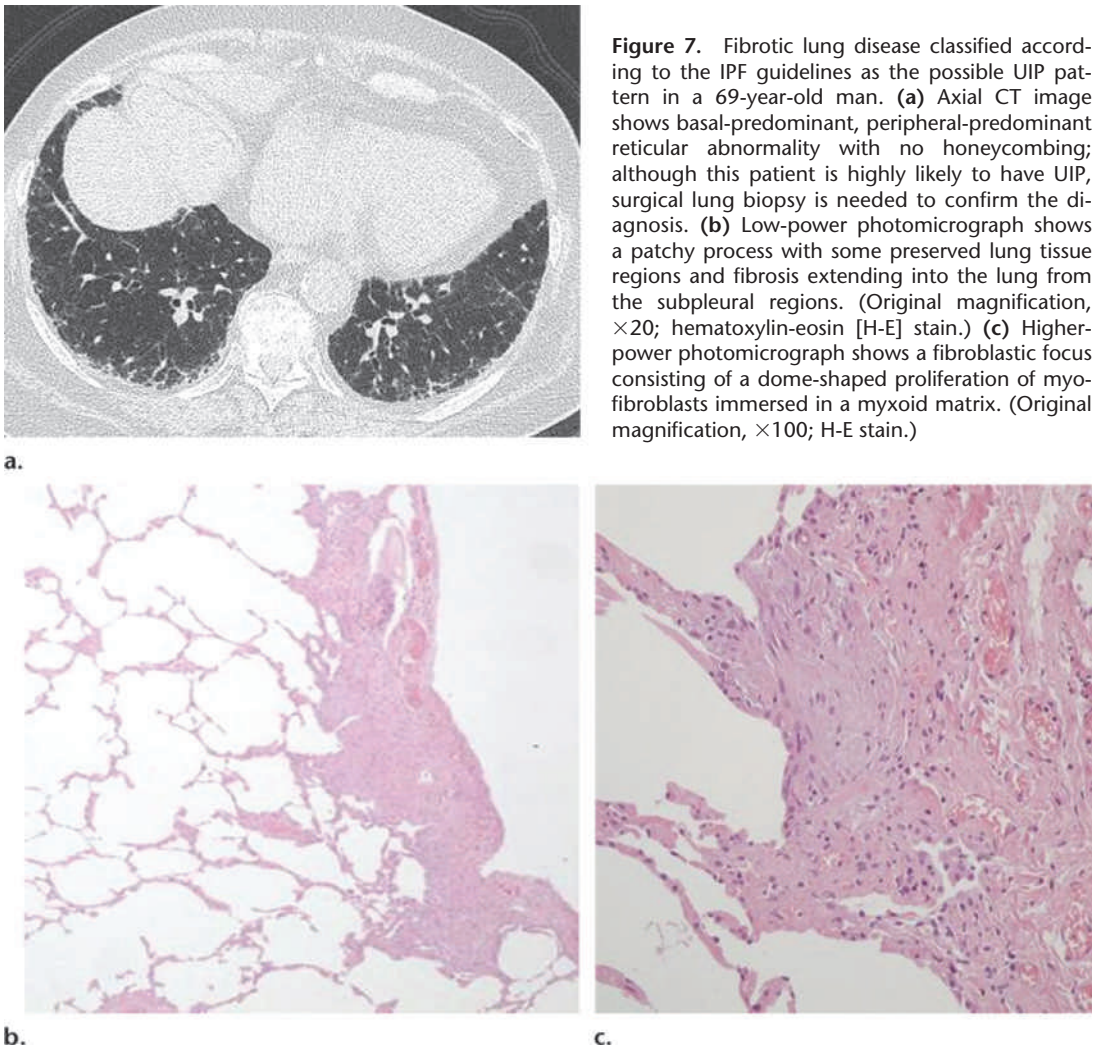

Figure 7. Fibrotic lung disease classified according to the IPF guidelines as the possible UIP pattern in a 69-year-old man. **(a)** Axial CT image shows basal-predominant, peripheral-predominant reticular abnormality with no honeycombing; although this patient is highly likely to have UIP, surgical lung biopsy is needed to confirm the diagnosis. **(b)** Low-power photomicrograph shows a patchy process with some preserved lung tissue regions and fibrosis extending into the lung from the subpleural regions. (Original magnification, ×20; hematoxylin-eosin [H-E] stain.) **(c)** Higher-power photomicrograph shows a fibroblastic focus consisting of a dome-shaped proliferation of myofibroblasts immersed in a myxoid matrix. (Original magnification, ×100; H-E stain.)

honeycombing, are highly likely to have UIP, suggesting that surgical lung biopsy may not be necessary in carefully selected cases of "possible UIP" (31,32). In addition, in patients whose CT images demonstrate neither a classic nor a possible UIP pattern, the specimen from surgical lung biopsy may still demonstrate the UIP pattern at histopathologic examination (28). Most of these atypical UIP cases are characterized by extensive areas of ground-glass opacity, whereas consolidation, nodules, or extensive areas of decreased attenuation can be seen less frequently (Fig 8) (16,17,19,33). The increasing recognition of atypical CT features of UIP is likely related in part to the fact that subjects with typical CT features of UIP now rarely undergo biopsy. Patients with IPF who have definite or possible UIP according to the CT criteria have a shorter survival than those who have indeterminate CT findings (16,19,23), and in some studies, subjects with possible UIP have a longer survival than those with definite UIP (19). The extent of disease and the presence of traction bronchiectasis and honeycombing on high-resolution CT images are also predictive of both survival and mortality in patients with IPF (26,34).

Mediastinal lymph node enlargement, usually mild, is evident at CT in approximately 70% of the patients with IPF (35). Coexisting emphysema is common and can sometimes make the diagnosis of IPF more difficult (24). Furthermore, describing the extent and severity of coexisting emphysema in patients with the UIP pattern has become important because of the effect of emphysema on the patient's clinical course, management, and prognosis (36,37). Occasionally, fine linear or small nodular foci of calcification are observed within areas of fibrosis as a result of ossification (38).

Longitudinal Evaluation.—Serial CT examinations in subjects with IPF generally show an increase in the extent and severity of fibrosis over months or years (39–41). As the disease progresses, it often appears to "creep" up the periphery of the lung, resulting in subpleural reticular

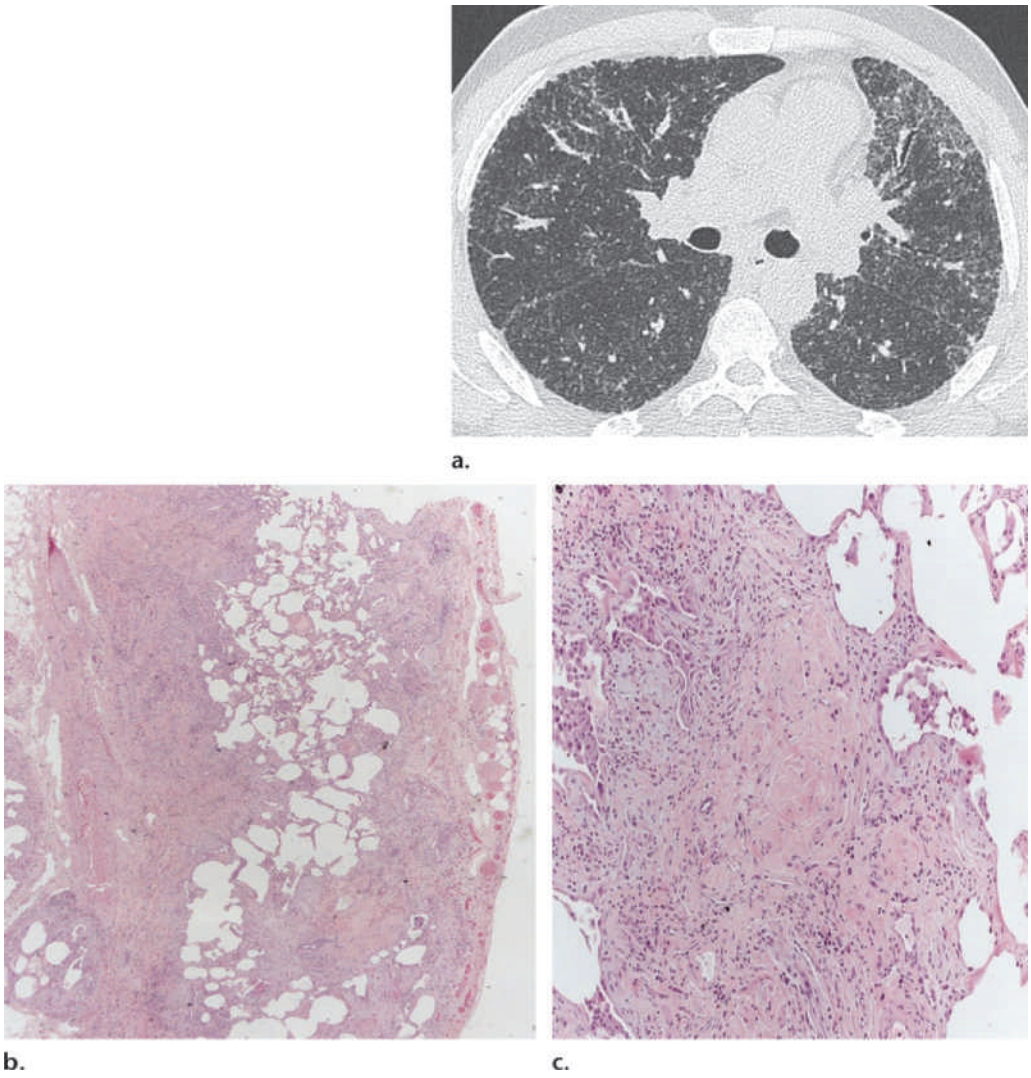

Figure 8. Fibrotic lung disease classified according to the IPF guidelines as a CT pattern inconsistent with UIP in a 37-year-old man. **(a)** Axial CT image shows that reticular abnormalities are so fine that they resemble micronodules (also involving the fissure), thus mimicking sarcoidosis. **(b)** However, a low-power photomicrograph shows histologic features of "definite UIP" that consist of abrupt alternating areas of scarred and normal lung. (Original magnification, ×20; H-E stain.) **(c)** Higher-power photomicrograph shows fibroblastic foci, another feature of definite UIP. (Original magnification, ×100; H-E stain.) The combined radiologic-pathologic features cause this case to be classified as possible UIP according to the IPF criteria (28).

opacities in the upper portions of the lungs. Some ground-glass opacities may improve or resolve with treatment; however, progression to reticulation and honeycombing is seen. Reticulation often progresses to honeycombing, and honeycomb cysts increase in extent and size (39,42). In subjects with either a possible or an inconsistent CT pattern for UIP, the pattern may evolve toward a definite UIP pattern (31). Recently, it has been shown that semiquantitative CT scoring for the extent of fibrosis or emphysema has prognostic value in the context of a clinical model that includes the *g*ender, *a*ge, and *p*hysiology (GAP model) for patients with IPF (43).

Radiologic Differential Diagnosis.—The primary role of CT is to separate chronic fibrosing lung diseases with a UIP pattern from those with non-UIP lesions, including those with findings associated with other IIPs (eg, RB-ILD, lymphoid interstitial pneumonia, and idiopathic pleuroparenchymal fibroelastosis) (Table 1). In more than 50% of patients suspected of having IPF/UIP, the presence of typical clinical and CT features of UIP, when identified by expert clinicians and radiologists, is sufficiently characteristic to allow a confident diagnosis and eliminate the need for surgical lung biopsy (28). A confident radiologic diagnosis of UIP at CT is correct in more than 90% of cases (44,45). However, as previously discussed, the diagnosis of honeycombing may be challenging, particularly in smokers who develop both lung fibrosis and emphysema. Akira et al (24) showed that in patients with concurrent em-

physema, the diagnosis was correct in 30 (44%) of 68 readings, including 20 (50%) for UIP and 10 (36%) for NSIP.

The UIP pattern can be found in asbestosis and connective tissue disease. In addition to the exposure history, the presence of pleural plaques or diffuse pleural thickening, subpleural dotlike or branching opacities, and less-coarse reticular shadows can help to distinguish asbestosis from IPF (46,47). In one study comparing pathologic and radiologic differences between IPF and UIP related to connective tissue disease, the latter had less emphysema and was more likely to have a nontypical UIP pattern without honeycombing (48).

Chronic hypersensitivity pneumonitis may also mimic IPF, but the former should be considered if poorly defined fine micronodules are seen, if there is multilobular decreased attenuation or airtrapping, or if there is sparing of the lung bases (33,49) (Fig 4). Patients with end-stage sarcoidosis may uncommonly develop a UIP-like pattern; however, sarcoidosis should be suspected if the cysts are large or if peribronchovascular nodules are present (50). Coal miners and silica-exposed workers may develop a chronic interstitial pneumonia with CT features similar to those of UIP (51). However, these cases tend to show less traction bronchiectasis, more subpleural homogeneous attenuation, and more random distribution of fibrosis than found in IPF/UIP (52).

In the findings from several case series of subjects with biopsy-proven UIP, 30%–60% of the IPF cases showed atypical CT appearances (16,17,23). Thus, in the correct clinical setting, a diagnosis of IPF is not excluded by thin-section CT appearances more suggestive of other interstitial lung diseases such as NSIP, chronic hypersensitivity pneumonitis, or sarcoidosis (Figs 7, 8) (17). In a study of 97 biopsy-proven IPF cases without honeycombing at CT and 38 cases with other IIPs, increasing age and increased profusion of reticular opacities at CT were found to predict a histopathologic confirmation of IPF at biopsy (53). In particular, subjects aged more than 65 or 70 years are highly likely to have UIP and are much less likely to have another IIP.

Idiopathic NSIP

Idiopathic NSIP is regarded as an uncommon but distinct entity among the IIPs. The NSIP pattern at CT occurs not only as an idiopathic condition, but also in a variety of settings (as outlined in the following section), and multidisciplinary discussion is especially important to establish the diagnosis of idiopathic NSIP (1,54). Surgical lung biopsy with a specimen showing the characteristic histologic features of NSIP is needed to secure a correct diagnosis. Although the prognosis of idiopathic NSIP is heterogeneous, it is however better than that of IPF.

CT Features.—Initially published descriptions of the CT appearances of NSIP varied widely, perhaps because of differing histopathologic diagnostic criteria (25,55–60). Although the radiologic and histologic NSIP pattern is commonly associated with an underlying cause (particularly connective tissue diseases, hypersensitivity pneumonitis, and drug toxicity), an American Thoracic Society workshop helped identify a more typical CT appearance of idiopathic NSIP (54). The CT features of idiopathic NSIP may vary according to the underlying proportion of inflammation (cellular component) and fibrosis. The reported high prevalence of a reticular pattern (87%), traction bronchiectasis (82%), and lobar volume loss (77%), as compared with the prevalence of ground-glass opacity (44%), is suggestive that that some degree of fibrosis is present in the vast majority of cases. In NSIP, honeycombing is absent or inconspicuous (41,54). Mildly enlarged mediastinal nodes are found in as many as 80% of cases (35).

In the craniocaudal plane, abnormalities are almost invariably predominant in the lower lobes (92%) and may be confined to the lower portions of the lungs, in contrast to the tendency of UIP to progressively involve the upper lungs. In the axial plane, either a peribronchovascular distribution or peripheral subpleural sparing is a classic feature of idiopathic NSIP (Fig 5) and is found in 21%–64% of cases (41,54).

Longitudinal Evaluation.—Although resolution of abnormalities may occur in a minority of patients with NSIP (Fig 5), most patients with NSIP have persistent abnormality (61). The extent of ground-glass attenuation decreases with time, but the extent of reticular abnormality persists (41,55), and the extent of honeycombing may increase (leading to a pattern suggestive of UIP) (41). Patients with CT findings compatible with NSIP and with NSIP confirmed at histologic examination have a longer survival than those with CT findings more compatible with UIP or an alternative diagnosis and with histologic findings of NSIP (62).

Radiologic Differential Diagnosis.—In previous reports, investigators have suggested that the accuracy of CT in differentiating NSIP from UIP was relatively low (56,59). However, as the characteristic imaging and pathologic features have become more recognized, the results of recent studies have shown a higher accuracy of CT in distinguishing NSIP and UIP. In a study of 21

cases of UIP and 32 cases of NSIP, investigators found that a CT diagnosis of NSIP was associated with a sensitivity of 70% and a specificity of 63% and suggested that NSIP can be distinguished from UIP in most but not all cases by the presence of prominent ground-glass attenuation (60). In the results of another study of 25 patients with surgical lung biopsy–proven NSIP and 22 patients with UIP, investigators found that the positive predictive value of a CT diagnosis made at intermediate or high confidence was 68% for NSIP and 88% for UIP (63). In this study, the presence of honeycombing as a predominant imaging finding was highly specific for UIP. In contrast, the presence of predominant ground-glass and reticular opacity was highly characteristic of NSIP, but some patients with UIP have this pattern and may require biopsy for differentiation from NSIP. In a study of 90 patients with biopsy-proven IIP, including 36 with NSIP and 11 with UIP, investigators reported that a high-confidence diagnosis of NSIP was correct in 65% of cases, compared with 91% for UIP (21). In this study, NSIP was misdiagnosed as UIP in 6.7% of patients, as cryptogenic organizing pneumonia in 6.7%, and as desquamative interstitial pneumonia or RB-ILD in 3.3%. Only a small percentage of patients with predominantly fibrotic NSIP showed overlap with the CT findings of UIP.

In another study of 92 patients with biopsy-proven IIP, including 20 with UIP, 16 with cellular NSIP, and 16 with fibrotic NSIP, observers made the correct diagnosis in 79% (64). Multivariate logistic regression analysis showed that the independent findings that distinguished UIP from cellular NSIP were the extent of honeycombing and the most proximal bronchus with traction bronchiectasis, and the finding that distinguished UIP from fibrotic NSIP was the extent of honeycombing. The results of other studies have shown a much lower prevalence of cellular NSIP (54). In a study of 66 patients with biopsy-proven chronic hypersensitivity pneumonitis, IPF, and NSIP, a confident diagnosis of NSIP was made in 53% and was correct in 94% (33). In this study, a general linear model showed that the features that best differentiated NSIP were relative subpleural sparing, absence of lobular areas with decreased attenuation, and lack of honeycombing. Differentiation of NSIP from UIP becomes more difficult in cigarette smokers with emphysema. In a study of 54 patients with NSIP and 42 patients with UIP, the CT diagnosis was correct in 44% of readings in those with concurrent emphysema, compared with 68% in those without concurrent emphysema (24).

The diagnosis of idiopathic NSIP requires meticulous clinical-radiologic-pathologic discussion. In the American Thoracic Society NSIP workshop, among 104 cases with a robust histopathologic diagnosis of NSIP, the findings from CT or clinical data resulted in a consensus diagnosis other than idiopathic NSIP in 38 (37%) of cases (54). Alternative diagnoses (most commonly, hypersensitivity pneumonitis) were favored by CT alone in 20% of cases, and in 14% of cases by clinical and CT data (54). Indeed, various ancillary CT findings may suggest a cause for an NSIP pattern (Table 4). In patients with NSIP related to connective tissue disease, the CT features often resemble or may even be indistinguishable from those of idiopathic NSIP (27). It is therefore important to look for additional abnormalities that may be suggestive of connective tissue disease, such as cysts, pericardial effusion, pleural disease (thickening or effusion), a dilated esophagus, mixed patterns of injury (NSIP and organizing pneumonia), or disproportionate pulmonary arterial enlargement (65).

Smoking-related IIPs

Respiratory Bronchiolitis–associated Interstitial Lung Disease

Respiratory bronchiolitis is the most common form of smoking-related lung injury and is usually asymptomatic. However, in a minority of cases, respiratory bronchiolitis is associated with clinical symptoms or physiologic abnormalities. In such cases, it is termed RB-ILD. A major change in clinical practice during the past decade is the greater reliance on CT findings and the clinical history, especially the smoking history, in making the diagnosis (1). At the time of the writing of the 2002 IIP American Thoracic Society–European Respiratory Society classification, this diagnosis of RB-ILD was reliant on the findings from surgical lung biopsy (2). Currently, in centers of expertise for IIP, this diagnosis is usually made largely on the basis of CT findings without surgical lung biopsy in the appropriate clinical setting.

CT Features.—The CT findings of RB-ILD are variable in terms of extent and combination of patterns. Key findings are inconspicuous poorly defined centrilobular nodules (upper lobe predominant), patchy ground-glass attenuation, scattered lobules of reduced attenuation (confirmed as lobular airtrapping at expiratory CT), and mild interlobular septal thickening (Fig 3, Table 1) (66,67). Ancillary findings are bronchial wall thickening and the presence of upper lobe centrilobular and paraseptal emphysema (rarely severe) (67). These findings may also be seen in asymptomatic cigarette smokers, albeit with less profu-

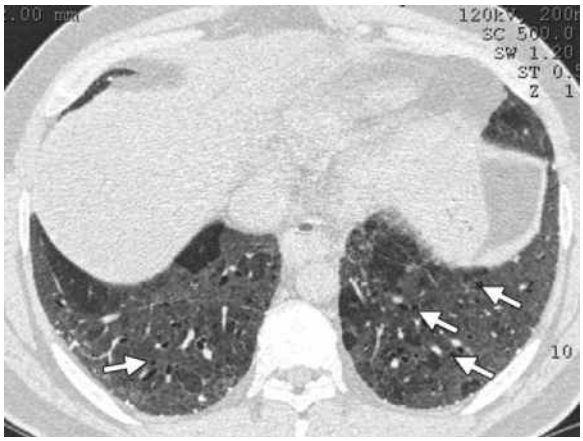

Figure 9. Desquamative interstitial pneumonia. Axial CT image shows areas of lower-lung–predominant ground-glass opacity with small cysts (arrows), findings that represent biopsy-proven desquamative interstitial pneumonia. Note that this was a rare case of desquamative interstitial pneumonia in a nonsmoker. Punctate subpleural calcifications are also depicted, which are presumably dystrophic calcification.

sion and severity than in symptomatic smokers with RB-ILD (68,69).

The findings from large-scale lung cancer CT screening studies have shown a noticeable prevalence of "interstitial abnormalities." The reported proportion of cigarette smokers, with or without chronic obstructive pulmonary disease, who have these interstitial abnormalities ranges from 1.3% to 9.7% (70–73). However, 1%–2% of these subjects have abnormalities with a more fibrotic appearance, which may progress with time (73). Lobular airtrapping, when present, is not usually as extensive as in other mixed interstitial and small airways diseases (74). There is no pathologic verification of these findings; however, it seems likely that most of these changes represent RB-ILD and smoking-related interstitial fibrosis (75,76).

Longitudinal Evaluation.—The longitudinal behavior of RB-ILD in cigarette smokers is not well documented but is likely heterogeneous (73). During a mean follow-up period of 5.5 years, Remy-Jardin et al (77) showed that centrilobular nodules in continuing smokers increased in profusion or were replaced by centrilobular emphysema; furthermore, ground-glass opacities and emphysema increased in prevalence in those who continued to smoke. The results of other studies have shown that centrilobular nodules are either stable or progressive in persistent smokers (71,78). However, in another study of a small group of patients with biopsy-proven RB-ILD who quit smoking, the CT findings of centrilobular nodules and ground-glass opacities regressed in all patients during a period of approximately 4 years, whereas fine reticular elements, traction bronchiolectasis, and emphysema did not (79).

Radiologic Differential Diagnosis.—The CT features of RB-ILD overlap with those of subacute hypersensitivity pneumonitis, desquamative interstitial pneumonia, and NSIP. The poorly defined centrilobular nodules of subacute hypersensitivity pneumonitis are often more profuse and diffuse than those of respiratory bronchiolitis and RB-ILD. Also, individuals with hypersensitivity pneumonitis are usually nonsmokers, and their fluid from bronchoalveolar lavage is characterized by lymphocytosis rather than pigment-laden macrophages. RB-ILD differs from desquamative interstitial pneumonia in that the ground-glass attenuation of RB-ILD is usually less extensive, patchier, and more poorly defined than that in desquamative interstitial pneumonia (Figs 3, 9) (80). Centrilobular nodules are uncommon or sparse in desquamative interstitial pneumonia. Furthermore, desquamative interstitial pneumonia–related abnormalities tend to predominate in the lower lobes, whereas those of RB-ILD are often predominantly distributed in the upper lobes (80). However, RB-ILD coexists with desquamative interstitial pneumonia (68,81).

Desquamative Interstitial Pneumonia

Desquamative interstitial pneumonia overlaps with RB-ILD in that the quality of the pigment-laden macrophages is identical, but their distribution and extent differ, with pigment-laden macrophages being more diffuse and extensive (within most of the distal airspaces) in desquamative interstitial pneumonia. Furthermore, the clinical presentation, imaging findings, and response to therapy differ, and RB-ILD and desquamative interstitial pneumonia remain classified separately (1).

CT Features.—Ground-glass opacification is the dominant pattern and has been depicted at CT in most, if not all, cases of desquamative interstitial pneumonia reported to date (82). The ground-glass pattern has a lower zone distribution in the majority of cases (73%), a subpleural distribution is found in 59% of cases, and the distribution is random in 23% (Table 1, Fig 9). In a few cases, the ground-glass opacification is entirely uniform and diffuse (18%). A limited reticular pattern and some irregular linear opacities, both usually basal, are frequent accompaniments (59%). Honeycombing is seen in less than one-third of cases and is usually peripheral and limited (80). Numerous small cystic airspaces, not to be confused with honeycomb destruction, may be present in areas of ground-glass opacification (83).

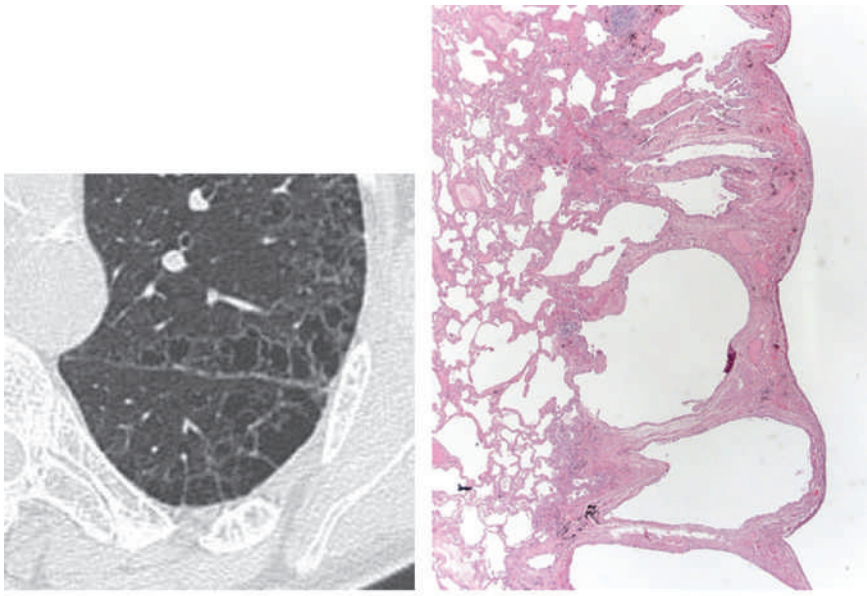

a. b.

Figure 10. Airspace enlargement with fibrosis. **(a)** Axial CT image shows thick-walled areas of centrilobular and paraseptal emphysema. **(b)** Low-power photomicrograph of the corresponding histologic specimen shows that the emphysematous holes are bounded by fibrotic abnormalities with a dense hyaline-like character. (Original magnification, ×20; H-E stain.)

Longitudinal Evaluation.—At follow-up CT of treated patients, there is usually partial or nearly complete resolution of areas of ground-glass opacification (84). Although the dominant feature of ground-glass opacification is generally reversible, the ground-glass opacification in some patients (<20%) remains fixed or even increases; in the absence of serial histopathologic specimens, it is uncertain what the persistent ground-glass pattern represents. Limited evidence in the literature and in the clinical experience with serial CT supports the idea that a substantial proportion of patients with desquamative interstitial pneumonia subsequently develop irreversible fibrosis, most frequently fibrotic NSIP (85).

Radiologic Differential Diagnosis.—In three studies including various IIPs, a correct first-choice diagnosis was made in 60%–70% of cases of desquamative interstitial pneumonia (21,59,64). Although ground-glass attenuation with lower and subpleural predominance at CT is characteristic in the cases of desquamative interstitial pneumonia, the CT appearances of desquamative interstitial pneumonia may overlap with those of RB-ILD; and, indeed, these entities may coexist along a spectrum of smoking-related lung injury (75). Desquamative interstitial pneumonia may usually be distinguished from NSIP by the absence of fibrotic features, such as traction bronchiectasis and lower lobe volume loss. A history of cigarette smoking and an abundance of macrophages in the specimen from bronchoalveolar lavage may also be helpful in supporting the diagnosis of desquamative interstitial pneumonia.

The IIP classification briefly mentions "airspace enlargement with fibrosis." Airspace enlargement with fibrosis is a smoking-related phenomenon not regarded as a distinct IIP, and the corresponding CT findings have not been well documented (1). Anecdotally, airspace enlargement with fibrosis differs from either RB-ILD or desquamative interstitial pneumonia because of the presence of more conspicuous reticular abnormalities admixed with emphysema (Fig 10) (75,76).

Acute or Subacute IIPs

Cryptogenic Organizing Pneumonia

Patients with cryptogenic organizing pneumonia usually present with a 4–6-week history of subacute influenza-like symptoms. Because many cases are secondary, use of the generic term *organizing pneumonia* for this reaction pattern is suggested, with modifiers as appropriate; for example, cryptogenic organizing pneumonia when idiopathic, or organizing pneumonia associated with any connective tissue disease or secondary to infection. At histologic examination, the organizing pneumonia pattern is a patchy process characterized primarily by buds of loose collagen-containing fibroblasts involving alveolar ducts and alveoli, with or without bronchiolar intraluminal polyps (1).

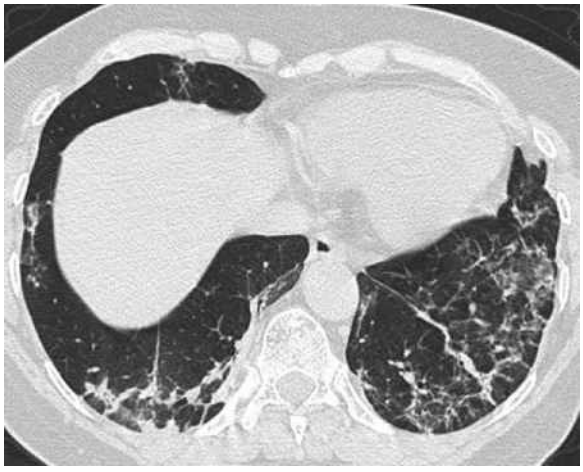

Figure 11. Perilobular pattern of organizing pneumonia. Axial CT image shows opacification around the periphery of individual secondary lobules, resembling poorly defined thickened interlobular septa.

CT Features.—The characteristic CT manifestations of cryptogenic organizing pneumonia consist of patchy unilateral or bilateral consolidation, which is usually a few centimeters in diameter and may contain air bronchograms with mild bronchial dilatation (86–88). Consolidation usually has a subpleural or peribronchial distribution with no craniocaudal predilection, although a basal predominance has been reported (87,89) (Fig 5c, Table 1). Randomly distributed ground-glass opacities are observed in 60%–86% of patients and usually coexist with consolidation (87–89). Occasionally, ground-glass opacities may be the predominant or only manifestation of cryptogenic organizing pneumonia at CT (87,89).

Since the 2002 American Thoracic Society–European Respiratory Society IIP classification document (2), two additional useful CT findings have been described in cryptogenic organizing pneumonia; perilobular opacities (Fig 11) and the reversed halo sign, or atoll sign, are encountered in 57% and 20% of cases, respectively, either isolated or more commonly in association with other findings (90,91). The identification of these two CT findings may be helpful in suggesting the diagnosis of cryptogenic organizing pneumonia. Irregular reticular opacities may be depicted but are rarely the major feature (92).

Several variant manifestations of cryptogenic organizing pneumonia have been described. Consolidation may be unifocal or cavitary, which makes the diagnosis more difficult (93,94); positron emission tomography may not be helpful because unifocal cryptogenic organizing pneumonia can be as hypermetabolic as lung cancer. Other less-common findings include multiple large nodular or masslike areas of consolidation, diffuse poorly defined micronodules, consolidation associated with satellite nodules, and band-like opacities with air bronchograms (90,95–97). A few enlarged mediastinal lymph nodes have been observed in 38% of cases (35). Small unilateral or bilateral pleural effusions may occur in 10%–30% of patients (86,87,91).

Longitudinal Evaluation.—Consolidation characteristically tends to migrate and may come and go, even without treatment (98). Cryptogenic organizing pneumonia manifesting as consolidation, ground-glass opacity, or nodules at CT frequently regresses with treatment, although there is a substantial relapse rate (87,88). It has been shown that in organizing pneumonia, areas of consolidation may be gradually replaced by a mixture of reticulation and ground-glass opacity that surrounds bronchiectatic airways, resembling an NSIP-like pattern (88,89,99) (Fig 5). Cryptogenic organizing pneumonia that manifests at CT as linear and reticular opacities frequently does not resolve after treatment and may evolve to fibrosis (89).

Radiologic Differential Diagnosis.—The radiologic differential diagnosis of cryptogenic organizing pneumonia in patients with areas of consolidation includes infection and aspiration. In the appropriate clinical context (consolidation increasing during several weeks despite therapy with antibiotics), a CT pattern of consolidation in a predominantly peribronchial or subpleural distribution is highly suggestive of cryptogenic organizing pneumonia. Bronchoalveolar lavage may be helpful to exclude infection (100). Other entities that may occasionally cause confusion include vasculitis, sarcoidosis, mucinous adenocarcinoma, and lymphoma (92). When the consolidation is subpleural, then the diagnosis of chronic eosinophilic pneumonia should be considered. However, the results of a study including 38 patients with cryptogenic organizing pneumonia and 43 patients with chronic eosinophilic pneumonia showed that the most helpful distinguishing feature of cryptogenic organizing pneumonia at CT was the presence of nodules, which were seen in 32% of patients with cryptogenic organizing pneumonia and only 5% of those with chronic eosinophilic pneumonia (101). Those patients who present with multiple large masses have a differential diagnosis that includes metastatic lung tumor, lymphoma, and pulmonary infection including septic emboli.

Acute Interstitial Pneumonia

Acute interstitial pneumonia is a rapidly progressive and histologically distinct form of IIP.

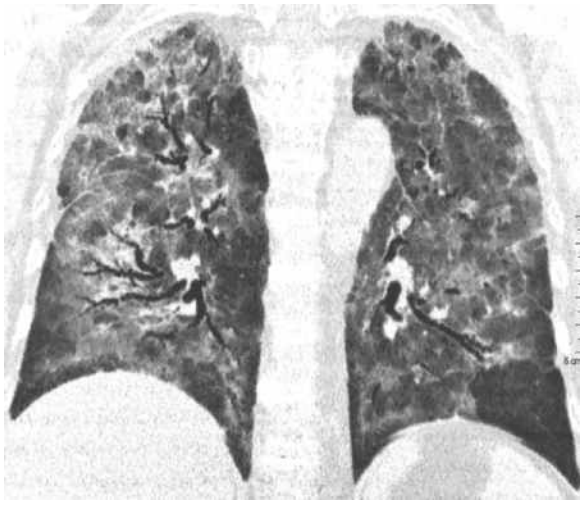

Figure 12. Acute interstitial pneumonia. Coronal reformatted CT image shows airways dilatation and distortion within areas of diffuse ground-glass opacity, findings suggestive that the disease is in the organizing stage. (Image courtesy of Giorgia Dalpiaz, MD, Bellaria Hospital, Bologna, Italy.)

The pathologic findings consist of an acute or organizing form of diffuse alveolar damage indistinguishable from the histologic pattern found in acute respiratory distress syndrome caused by sepsis and shock (1).

CT Features.—The most common findings at CT in patients with acute interstitial pneumonia are areas of ground-glass attenuation, bronchial dilatation, and architectural distortion (102). The extent of the areas of ground-glass attenuation correlates with disease duration. In the early exudative phase, the lung shows areas of ground-glass attenuation that are most often bilateral and patchy, with areas of focal sparing of lung lobules giving a geographic appearance (103) (Fig 12). The ground-glass opacities are neither distinctly subpleural nor central. Consolidation is seen in the majority of cases. The distribution is most often basilar but can occasionally be diffuse or, rarely, have an upper lobe predominance (Table 1). In patients with classic acute interstitial pneumonia, the areas of consolidation are most often in the dependent areas of lung, a finding that is suggestive of alveolar closure from the weight and hydrostatic pressure of the more-superior lung tissue. The later organizing stage of acute interstitial pneumonia is associated with distortion of bronchovascular bundles, traction bronchiectasis, and honeycombing (Fig 12). The areas of consolidation tend to be replaced by ground-glass opacities. Cysts and other lucent areas of lung become more common in the late stages of acute interstitial pneumonia (102).

Longitudinal Evaluation.—Because of the relatively poor prognosis of acute interstitial pneumonia, there has been no systematic evaluation of the longitudinal CT findings in this condition. The few patients who survive show progressive clearing of the ground-glass attenuation and consolidation. The most common residual CT findings are areas of hypoattenuation, lung cysts, reticular abnormality, and associated parenchymal distortion occurring mainly in the nondependent (anterior) portion of the lung (104).

CT assessment is potentially helpful in predicting patient prognosis (105). In a scoring system established by Ichikado et al (105,106), CT findings were graded on a scale of 1–6, with areas graded as follows: 1, normal attenuation; 2, ground-glass attenuation, 3, airspace consolidation; 4, ground-glass attenuation associated with traction bronchiolectasis or bronchiectasis; 5, airspace consolidation associated with traction bronchiolectasis or bronchiectasis; and 6, honeycombing. An overall score was obtained by quantifying the extent of each abnormality in three lung zones in each lung. Overall CT scores of survivors were significantly lower than those of nonsurvivors (P = .0003) (105). In addition, the CT score was independently associated with mortality (106).

Radiologic Differential Diagnosis.—Although the CT features of acute interstitial pneumonia are similar to those of acute respiratory distress syndrome, patients with acute interstitial pneumonia are more likely to have a symmetric bilateral distribution with lower lung predominance, compared with patients with acute respiratory distress syndrome (107). Sometimes, especially in the early stage, the findings of acute interstitial pneumonia may be similar to cryptogenic organizing pneumonia, with areas of airspace consolidation. In the results of a study of 27 patients with acute interstitial pneumonia and 14 with cryptogenic organizing pneumonia, investigators reported that traction bronchiectasis, interlobular septal thickening, and intralobular reticular opacities were significantly more prevalent in

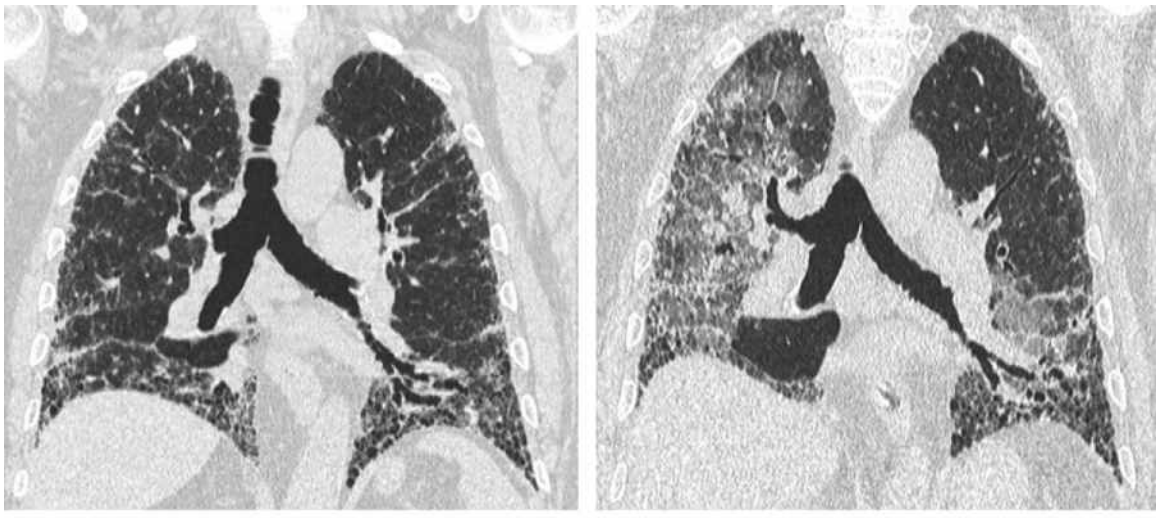

a. b.

Figure 13. Acute exacerbation of IPF. **(a)** Coronal baseline CT image shows coarse subpleural reticulation and honeycombing. **(b)** Coronal CT image obtained 6 months later, when the patient complained of 10 days of progressive breathlessness, shows areas of patchy ground-glass opacity superimposed on the reticular abnormality, as well as within the previously relatively normal lung parenchyma.

acute interstitial pneumonia than in cryptogenic organizing pneumonia ($P < .01$) (108).

The radiologic differential diagnosis of acute interstitial pneumonia depends on the stage but can include widespread infection (particularly *Pneumocystis jiroveci* pneumonia), hydrostatic edema, acute eosinophilic pneumonia, diffuse pulmonary hemorrhage, acute hypersensitivity pneumonitis, and alveolar proteinosis. In the findings from a study of 90 patients with acute parenchymal lung diseases, including 21 with acute interstitial pneumonia, investigators showed that a correct first-choice diagnosis was made in 90% of cases of acute interstitial pneumonia (109). Widely distributed traction bronchiectasis is a clue for the differentiation of acute interstitial pneumonia from other acute parenchymal lung diseases. The presence of substantial interlobular septal thickening and pleural effusions should be suggestive of acute eosinophilic pneumonia or pulmonary edema (110). Profuse centrilobular nodules or mosaic attenuation should be suggestive of hypersensitivity pneumonitis.

Acute Exacerbation of IIP

Acute exacerbation (also termed the *accelerated phase*) causes an acute respiratory worsening of any chronic IIP. Histologically, acute exacerbation of IIP manifests as acute or organizing diffuse alveolar damage and should be suspected in patients with IPF with extensive or rapidly progressive new ground-glass opacities at CT (Fig 13). Importantly, the new parenchymal opacities may be caused by infection or heart failure that must be excluded to secure the diagnosis of acute exacerbation of IIP (111). Often, these subjects undergo CT to exclude pulmonary embolism as a cause of acutely progressive hypoxia. Three CT patterns have been described: peripheral, multifocal, and diffuse parenchymal opacification (predominantly ground-glass opacity but sometimes consolidation), all occurring against a background of preexisting fibrotic change typical of UIP/IPF (112). Akira et al (112) found that patients with the diffuse pattern of parenchymal opacification at CT had a higher risk of death than those with the multifocal or peripheral pattern. However, in the results of another study, other investigators showed that both the pathologic findings and the CT score were more predictive in terms of prognosis than the CT pattern itself (113).

Acute exacerbations of other fibrotic lung diseases, including idiopathic NSIP, have also been described. Some have suggested that the outcome of acute exacerbation in NSIP may be better than that in UIP (114,115).

Rare IIPs

Lymphoid Interstitial Pneumonia

Lymphoid interstitial pneumonia is a benign lymphoproliferative condition characterized by a dense interstitial lymphoid infiltrate. Because most cases of lymphoid interstitial pneumonia are associated with other conditions, true idiopathic lymphoid interstitial pneumonia is rare (1).

CT Features.—Common CT findings in lymphoid interstitial pneumonia are areas of ground-glass opacities, nodules of varying sizes (which may be ill-defined), interlobular septal thickening,

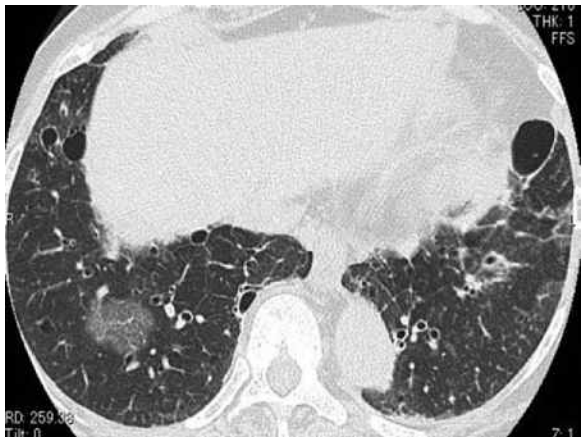

Figure 14. Lymphoid interstitial pneumonia. Axial CT image shows perivascular cysts of varying size and areas of patchy ground-glass opacity in the lower lobes. Cylindrical bronchiectasis is also depicted.

thickened bronchovascular bundles, and thin-walled cysts (1–30 mm) (Table 1). CT findings of lymphoid interstitial pneumonia overlap with those of cellular NSIP because of its frequent lower lobe predominance and areas of ground-glass attenuation, derived from the extensive alveolar septal infiltration of lymphoid cells (116,117). However, cyst formation is more common and extensive in lymphoid interstitial pneumonia than in cellular NSIP (Fig 14) and may, in fact, be the only finding. The cysts in lymphoid interstitial pneumonia are usually discrete and sometimes clustered and tend to be peribronchovascular in distribution (116).

Longitudinal Evaluation.—Follow-up CT studies show that the ground-glass opacity improves in the majority of cases of lymphoid interstitial pneumonia, although cysts remain, with rare cases developing honeycomb change (118).

Radiologic Differential Diagnosis.—If the patients with lymphoid interstitial pneumonia have multiple cysts depicted at high-resolution CT, the differential diagnosis includes Langerhans cell histiocytosis, lymphangioleiomyomatosis, emphysema, and desquamative interstitial pneumonia. However, in contrast to these other entities, the cysts of lymphoid interstitial pneumonia usually predominate in the lower portions of the lungs and around bronchi and vessels. Furthermore, ground-glass opacity and reticulation are associated findings that help differentiate lymphoid interstitial pneumonia from either lymphangioleiomyomatosis or Langerhans cell histiocytosis, in which none of these findings are conspicuous. In the results of a study of 92 patients with chronic cystic lung diseases, including 16 subjects with lymphoid interstitial pneumonia, investigators reported that the correct diagnosis was made in 81% of the cases of lymphoid interstitial pneumonia (83).

Idiopathic Pleuroparenchymal Fibroelastosis

Idiopathic pleuroparenchymal fibroelastosis is a rare condition that consists of a form of fibrosis rich in elastic fibers that involves the pleura and subpleural lung parenchyma, predominantly in the upper lobes. Disease progression occurs in 60% of patients, with death from the disease in 40% (1).

CT Features.—CT appearances of idiopathic pleuroparenchymal fibroelastosis are distinctive, with irregular pleural thickening and "tags" in the upper zones that merge with fibrotic changes in the subjacent lung, associated with evidence of substantial upper lobe volume loss (architectural distortion, traction bronchiectasis, and hilar elevation) (Table 1; Figs 2, 15) (119). In the results of a study by Reddy et al (120), fibrotic CT features remote from the pleuroparenchymal changes (ie, in the mid and lower lung zones) were depicted in five of 12 cases (42%). Most of these fibrotic abnormalities were more reminiscent of an NSIP pattern at CT, although the results from lung biopsy disclosed UIP findings for some of these cases (120).

Longitudinal Evaluation.—Few data are available on the longitudinal behavior of idiopathic pleuroparenchymal fibroelastosis. The findings from serial CT studies demonstrated stability or minor progression with respect to the pleuroparenchymal changes. However, marked progression during a few months has been also described (120,121).

Differential Diagnosis.—The differential diagnosis generally includes familial pulmonary fibrosis, connective tissue disease (particularly ankylosing spondylitis), fibrotic sarcoidosis, and chronic hypersensitivity pneumonitis. However, the striking apical subpleural predominance and associated

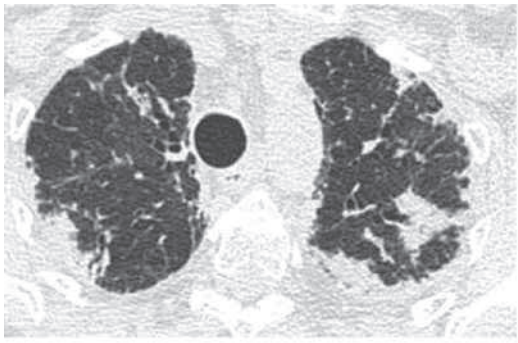

a.

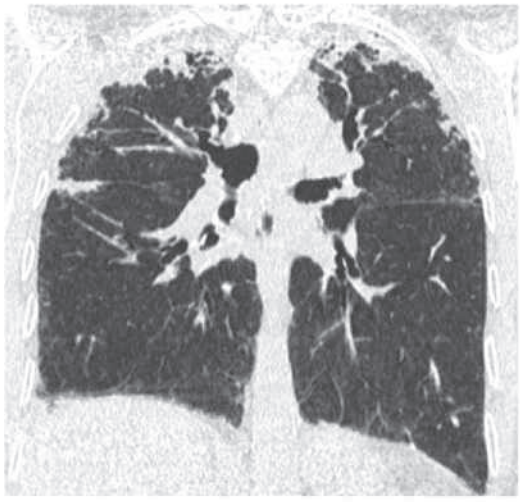

b.

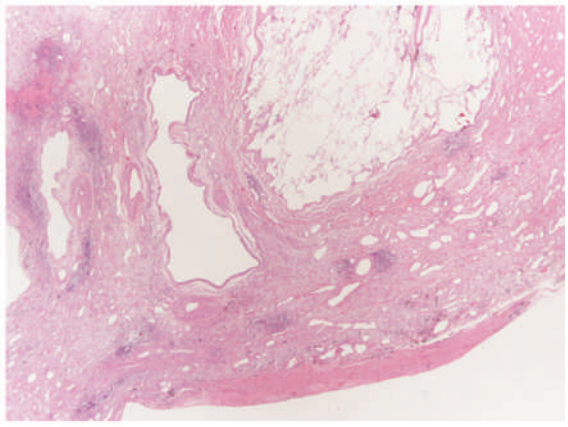

c.

Figure 15. Idiopathic pleuroparenchymal fibroelastosis. **(a, b)** Axial CT image **(a)** through the upper zones and coronal reformatted CT image **(b)** show typical features of idiopathic pleuroparenchymal fibroelastosis, with bilateral irregular pleural thickening and a subjacent reticular pattern consistent with fibrosis. **(c)** Low-power photomicrograph of the histologic specimen shows pleural thickening and subpleural fibrosis. (Original magnification, ×20; H-E stain.) (Fig 15c courtesy of Alberto Cavazza, MD, Azienda Ospedaliera S. Maria Nuova, Reggio Emilia, Italy.)

pleural thickening will usually help distinguish idiopathic pleuroparenchymal fibroelastosis from the other entities, although some cases of chronic hypersensitivity pneumonitis may appear identical.

Unclassifiable IIP

The 2013 IIP consensus statement acknowledges, as did the 2002 consensus statement, that a final diagnosis is not always achievable (1,2). The frequency of "unclassifiable" cases will vary among centers, but these cases account for a substantial amount of discussion time by the multidisciplinary team—the management of such cases may be aided by the disease behavior classification (Table 2). In the results of a study from a single center, investigators reported that unclassifiable interstitial lung disease accounted for 10% of their cohort of cases of interstitial lung disease (122). Patients were considered to have unclassifiable interstitial lung disease if a prospective review of clinical, radiologic, and pathologic data did not reveal a specific diagnosis after multidisciplinary discussion. The most common reason for a case being designated as unclassifiable was a missing histopathologic assessment because of the high risk associated with surgical lung biopsy (52%).

With regard to the CT features, the definite UIP pattern was found at CT in 17% of patients with unclassifiable ILD, and the "possible UIP pattern" was found in 50% (122). However, there were other compelling clinical, physiologic, or histologic features that made a definite diagnosis not possible. Independent predictors of survival in patients with unclassifiable interstitial lung disease included the diffusing capacity of the lung for carbon monoxide and a radiologic fibrosis score at CT examination. In subjects with unclassifiable interstitial lung disease, the CT features of fibrosis (ie, honeycombing, traction bronchiectasis) are suggestive of a poor prognosis, similar to that in patients with confirmed IPF. Whether unclassifiable cases actually represent patients with atypical IPF or remain a heterogeneous collection of ill-defined conditions requires further study.

Summary

The revision of the IIP classification has provided incremental but important advances in the understanding of IIPs and other interstitial lung diseases. A systematic approach to chest CT in patients suspected of having IIP entails the need for thin-section CT, evaluation of image quality, precise description of specific disease features with

standard terminology, and determination of the disease distribution in the axial and craniocaudal planes. Radiologists should first distinguish fibrosing from nonfibrosing entities. The main CT differential diagnosis of fibrosing lung disease is between the definite or possible UIP pattern and other fibrotic patterns such as NSIP and chronic hypersensitivity pneumonitis. Two new entities have also been included in the latest IIP classification: *(a)* Although rare, idiopathic pleuroparenchymal fibroelastosis displays typical CT features, and its diagnosis is increasingly suggested by radiologists. *(b)* The designation of unclassifiable IIP results from a prospective review of clinical, radiologic, and pathologic data that did not disclose a specific diagnosis after multidisciplinary discussion. Furthermore, the progression of the IIPs may be heterogeneous, and radiologists are often challenged by the interpretation of progressive changes and acute complications.

***Disclosures of Conflicts of Interest.*—D.A.L.** *Activities related to the present article:* disclosed no relevant relationships. *Activities not related to the present article:* research support from Siemens and Parexel Imaging; consultant to Parexel Imaging, Boehringer Ingelheim, Genentech, Gilead, and Intermune. *Other activities:* disclosed no relevant relationships. **D.M.H.** *Activities related to the present article:* disclosed no relevant relationships. *Activities not related to the present article:* support from AstraZeneca, Boehringer Ingelheim, GlaxoSmithKline, and Intermune. *Other activities:* disclosed no relevant relationships.

References

1. Travis WD, Costabel U, Hansell DM, et al. An official American Thoracic Society/European Respiratory Society statement: update of the international multidisciplinary classification of the idiopathic interstitial pneumonias. Am J Respir Crit Care Med 2013;188(6):733–748.
2. American Thoracic Society; European Respiratory Society. American Thoracic Society/European Respiratory Society International Multidisciplinary Consensus Classification of the Idiopathic Interstitial Pneumonias. Am J Respir Crit Care Med 2002;165(2):277–304.
3. Mayo JR. CT evaluation of diffuse infiltrative lung disease: dose considerations and optimal technique. J Thorac Imaging 2009;24(4):252–259.
4. Dodd JD, de Jong PA, Levy RD, Coxson HO, Mayo JR. Conventional high-resolution CT versus contiguous multidetector CT in the detection of bronchiolitis obliterans syndrome in lung transplant recipients. J Thorac Imaging 2008;23(4):235–243.
5. Remy-Jardin M, Campistron P, Amara A, et al. Usefulness of coronal reformations in the diagnostic evaluation of infiltrative lung disease. J Comput Assist Tomogr 2003;27(2):266–273.
6. Johkoh T, Sakai F, Noma S, et al. Honeycombing on CT: its definition, pathologic correlation, and future direction of its diagnosis. Eur J Radiol 2014;83(1):27–31.
7. Hodnett PA, Naidich DP. Fibrosing interstitial lung disease: a practical high-resolution computed tomography-based approach to diagnosis and management and a review of the literature. Am J Respir Crit Care Med 2013;188(2):141–149.
8. Singh S, Kalra MK, Ali Khawaja RD, et al. Radiation dose optimization and thoracic computed tomography. Radiol Clin North Am 2014;52(1):1–15.
9. Christe A, Charimo-Torrente J, Roychoudhury K, Vock P, Roos JE. Accuracy of low-dose computed tomography (CT) for detecting and characterizing the most common CT-patterns of pulmonary disease. Eur J Radiol 2013;82(3):e142–e150. http://www.ejradiology.com/article/S0720-048X(12)00480-9/abstract. Published November 5, 2012. Accessed February 1, 2015.
10. Hansell DM. Thin-section CT of the lungs: the hinterland of normal. Radiology 2010;256(3):695–711.
11. Tokura S, Okuma T, Akira M, Arai T, Inoue Y, Kitaichi M. Utility of expiratory thin-section CT for fibrotic interstitial pneumonia. Acta Radiol 2014;55(9):1050–1055.
12. Gotway MB, Lee ES, Reddy GP, Golden JA, Webb WR. Low-dose, dynamic, expiratory thin-section CT of the lungs using a spiral CT scanner. J Thorac Imaging 2000;15(3):168–172.
13. Hansell DM, Bankier AA, MacMahon H, McLoud TC, Müller NL, Remy J. Fleischner Society: glossary of terms for thoracic imaging. Radiology 2008;246(3):697–722.
14. Walsh SL, Hansell DM. Diffuse interstitial lung disease: overlaps and uncertainties. Eur Radiol 2010;20(8):1859–1867.
15. Watadani T, Sakai F, Johkoh T, et al. Interobserver variability in the CT assessment of honeycombing in the lungs. Radiology 2013;266(3):936–944.
16. Sumikawa H, Johkoh T, Colby TV, et al. Computed tomography findings in pathological usual interstitial pneumonia: relationship to survival. Am J Respir Crit Care Med 2008;177(4):433–439.
17. Sverzellati N, Wells AU, Tomassetti S, et al. Biopsy-proved idiopathic pulmonary fibrosis: spectrum of nondiagnostic thin-section CT diagnoses. Radiology 2010;254(3):957–964.
18. Thomeer M, Demedts M, Behr J, et al. Multidisciplinary interobserver agreement in the diagnosis of idiopathic pulmonary fibrosis. Eur Respir J 2008;31(3):585–591.
19. Flaherty KR, Thwaite EL, Kazerooni EA, et al. Radiological versus histological diagnosis in UIP and NSIP: survival implications. Thorax 2003;58(2):143–148.
20. Aziz ZA, Wells AU, Hansell DM, et al. HRCT diagnosis of diffuse parenchymal lung disease: inter-observer variation. Thorax 2004;59(6):506–511.
21. Tsubamoto M, Müller NL, Johkoh T, et al. Pathologic subgroups of nonspecific interstitial pneumonia: differential diagnosis from other idiopathic interstitial pneumonias on high-resolution computed tomography. J Comput Assist Tomogr 2005;29(6):793–800.
22. Flaherty KR, Andrei AC, King TE Jr, et al. Idiopathic interstitial pneumonia: do community and academic physicians agree on diagnosis? Am J Respir Crit Care Med 2007;175(10):1054–1060.
23. Lynch DA, Godwin JD, Safrin S, et al. High-resolution computed tomography in idiopathic pulmonary fibrosis: diagnosis and prognosis. Am J Respir Crit Care Med 2005;172(4):488–493.
24. Akira M, Inoue Y, Kitaichi M, Yamamoto S, Arai T, Toyokawa K. Usual interstitial pneumonia and nonspecific interstitial pneumonia with and without concurrent emphysema: thin-section CT findings. Radiology 2009;251(1):271–279.
25. Johkoh T, Müller NL, Colby TV, et al. Nonspecific interstitial pneumonia: correlation between thin-section CT findings and pathologic subgroups in 55 patients. Radiology 2002;225(1):199–204.
26. Edey AJ, Devaraj AA, Barker RP, Nicholson AG, Wells AU, Hansell DM. Fibrotic idiopathic interstitial pneumonias: HRCT findings that predict mortality. Eur Radiol 2011;21(8):1586–1593.
27. Walsh SL, Sverzellati N, Devaraj A, Keir GJ, Wells AU, Hansell DM. Connective tissue disease related fibrotic lung disease: high resolution computed tomographic and pulmonary function indices as prognostic determinants. Thorax 2014;69(3):216–222.
28. Raghu G, Collard HR, Egan JJ, et al. An official ATS/ERS/JRS/ALAT statement: idiopathic pulmonary fibrosis—evidence-based guidelines for diagnosis and management. Am J Respir Crit Care Med 2011;183(6):788–824.
29. Fernández Pérez ER, Daniels CE, Schroeder DR, et al. Incidence, prevalence, and clinical course of idiopathic pulmonary fibrosis: a population-based study. Chest 2010;137(1):129–137.

30. Tcherakian C, Cottin V, Brillet PY, et al. Progression of idiopathic pulmonary fibrosis: lessons from asymmetrical disease. Thorax 2011;66(3):226–231.
31. Gruden JF, Panse PM, Leslie KO, Tazelaar HD, Colby TV. UIP diagnosed at surgical lung biopsy, 2000-2009: HRCT patterns and proposed classification system. AJR Am J Roentgenol 2013;200(5):W458–W467.
32. Raghu G, Lynch D, Godwin JD, et al. Diagnosis of idiopathic pulmonary fibrosis with high-resolution CT in patients with little or no radiological evidence of honeycombing: secondary analysis of a randomised, controlled trial. Lancet Respir Med 2014;2(4):277–284.
33. Silva CI, Müller NL, Lynch DA, et al. Chronic hypersensitivity pneumonitis: differentiation from idiopathic pulmonary fibrosis and nonspecific interstitial pneumonia by using thin-section CT. Radiology 2008;246(1): 288–297.
34. Shin KM, Lee KS, Chung MP, et al. Prognostic determinants among clinical, thin-section CT, and histopathologic findings for fibrotic idiopathic interstitial pneumonias: tertiary hospital study. Radiology 2008;249(1):328–337.
35. Souza CA, Müller NL, Lee KS, Johkoh T, Mitsuhiro H, Chong S. Idiopathic interstitial pneumonias: prevalence of mediastinal lymph node enlargement in 206 patients. AJR Am J Roentgenol 2006;186(4):995–999.
36. Mejía M, Carrillo G, Rojas-Serrano J, et al. Idiopathic pulmonary fibrosis and emphysema: decreased survival associated with severe pulmonary arterial hypertension. Chest 2009;136(1):10–15.
37. Kurashima K, Takayanagi N, Tsuchiya N, et al. The effect of emphysema on lung function and survival in patients with idiopathic pulmonary fibrosis. Respirology 2010; 15(5):843–848.
38. Kim TS, Han J, Chung MP, Chung MJ, Choi YS. Disseminated dendriform pulmonary ossification associated with usual interstitial pneumonia: incidence and thin-section CT-pathologic correlation. Eur Radiol 2005;15(8):1581–1585.
39. Akira M, Sakatani M, Ueda E. Idiopathic pulmonary fibrosis: progression of honeycombing at thin-section CT. Radiology 1993;189(3):687–691.
40. Jeong YJ, Lee KS, Müller NL, et al. Usual interstitial pneumonia and non-specific interstitial pneumonia: serial thin-section CT findings correlated with pulmonary function. Korean J Radiol 2005;6(3):143–152.
41. Silva CI, Müller NL, Hansell DM, Lee KS, Nicholson AG, Wells AU. Nonspecific interstitial pneumonia and idiopathic pulmonary fibrosis: changes in pattern and distribution of disease over time. Radiology 2008;247(1):251–259.
42. Terriff BA, Kwan SY, Chan-Yeung MM, Müller NL. Fibrosing alveolitis: chest radiography and CT as predictors of clinical and functional impairment at follow-up in 26 patients. Radiology 1992;184(2):445–449.
43. Ley B, Elicker BM, Hartman TE, et al. Idiopathic pulmonary fibrosis: CT and risk of death. Radiology 2014;273(2):570–579.
44. Hunninghake GW, Zimmerman MB, Schwartz DA, et al. Utility of a lung biopsy for the diagnosis of idiopathic pulmonary fibrosis. Am J Respir Crit Care Med 2001;164(2):193–196.
45. Raghu G, Mageto YN, Lockhart D, Schmidt RA, Wood DE, Godwin JD. The accuracy of the clinical diagnosis of new-onset idiopathic pulmonary fibrosis and other interstitial lung disease: a prospective study. Chest 1999;116(5):1168–1174.
46. Akira M, Yamamoto S, Inoue Y, Sakatani M. High-resolution CT of asbestosis and idiopathic pulmonary fibrosis. AJR Am J Roentgenol 2003;181(1):163–169.
47. Copley SJ, Wells AU, Sivakumaran P, et al. Asbestosis and idiopathic pulmonary fibrosis: comparison of thin-section CT features. Radiology 2003;229(3):731–736.
48. Song JW, Do KH, Kim MY, Jang SJ, Colby TV, Kim DS. Pathologic and radiologic differences between idiopathic and collagen vascular disease-related usual interstitial pneumonia. Chest 2009;136(1):23–30.
49. Morell F, Villar A, Montero MA, et al. Chronic hypersensitivity pneumonitis in patients diagnosed with idiopathic pulmonary fibrosis: a prospective case-cohort study. Lancet Respir Med 2013;1(9):685–694.
50. Padley SP, Padhani AR, Nicholson A, Hansell DM. Pulmonary sarcoidosis mimicking cryptogenic fibrosing alveolitis on CT. Clin Radiol 1996;51(11):807–810.
51. Katabami M, Dosaka-Akita H, Honma K, et al. Pneumoconiosis-related lung cancers: preferential occurrence from diffuse interstitial fibrosis-type pneumoconiosis. Am J Respir Crit Care Med 2000;162(1):295–300.
52. Arakawa H, Johkoh T, Honma K, et al. Chronic interstitial pneumonia in silicosis and mix-dust pneumoconiosis: its prevalence and comparison of CT findings with idiopathic pulmonary fibrosis. Chest 2007;131(6):1870–1876.
53. Fell CD, Martinez FJ, Liu LX, et al. Clinical predictors of a diagnosis of idiopathic pulmonary fibrosis. Am J Respir Crit Care Med 2010;181(8):832–837.
54. Travis WD, Hunninghake G, King TE Jr, et al. Idiopathic nonspecific interstitial pneumonia: report of an American Thoracic Society project. Am J Respir Crit Care Med 2008;177(12):1338–1347.
55. Kim EY, Lee KS, Chung MP, Kwon OJ, Kim TS, Hwang JH. Nonspecific interstitial pneumonia with fibrosis: serial high-resolution CT findings with functional correlation. AJR Am J Roentgenol 1999;173(4):949–953.
56. Hartman TE, Swensen SJ, Hansell DM, et al. Nonspecific interstitial pneumonia: variable appearance at high-resolution chest CT. Radiology 2000;217(3):701–705. [Published correction appears in Radiology 2001;218(2):606.]
57. Park JS, Lee KS, Kim JS, et al. Nonspecific interstitial pneumonia with fibrosis: radiographic and CT findings in seven patients. Radiology 1995;195(3):645–648.
58. Nagai S, Kitaichi M, Itoh H, Nishimura K, Izumi T, Colby TV. Idiopathic nonspecific interstitial pneumonia/fibrosis: comparison with idiopathic pulmonary fibrosis and BOOP. Eur Respir J 1998;12(5):1010–1019.
59. Johkoh T, Müller NL, Cartier Y, et al. Idiopathic interstitial pneumonias: diagnostic accuracy of thin-section CT in 129 patients. Radiology 1999;211(2):555–560.
60. MacDonald SL, Rubens MB, Hansell DM, et al. Nonspecific interstitial pneumonia and usual interstitial pneumonia: comparative appearances at and diagnostic accuracy of thin-section CT. Radiology 2001;221(3):600–605.
61. Nishiyama O, Kondoh Y, Taniguchi H, et al. Serial high resolution CT findings in nonspecific interstitial pneumonia/fibrosis. J Comput Assist Tomogr 2000;24(1):41–46.
62. Akira M, Inoue Y, Arai T, Okuma T, Kawata Y. Long-term follow-up high-resolution CT findings in non-specific interstitial pneumonia. Thorax 2011;66(1):61–65.
63. Elliot TL, Lynch DA, Newell JD Jr, et al. High-resolution computed tomography features of nonspecific interstitial pneumonia and usual interstitial pneumonia. J Comput Assist Tomogr 2005;29(3):339–345.
64. Sumikawa H, Johkoh T, Ichikado K, et al. Usual interstitial pneumonia and chronic idiopathic interstitial pneumonia: analysis of CT appearance in 92 patients. Radiology 2006;241(1):258–266.
65. Hwang JH, Misumi S, Sahin H, Brown KK, Newell JD, Lynch DA. Computed tomographic features of idiopathic fibrosing interstitial pneumonia: comparison with pulmonary fibrosis related to collagen vascular disease. J Comput Assist Tomogr 2009;33(3):410–415.
66. Remy-Jardin M, Remy J, Gosselin B, Becette V, Edme JL. Lung parenchymal changes secondary to cigarette smoking: pathologic-CT correlations. Radiology 1993;186(3): 643–651.
67. Park JS, Brown KK, Tuder RM, Hale VA, King TE Jr, Lynch DA. Respiratory bronchiolitis-associated interstitial lung disease: radiologic features with clinical and pathologic correlation. J Comput Assist Tomogr 2002;26(1): 13–20.
68. Wells AU, Nicholson AG, Hansell DM. Challenges in pulmonary fibrosis. IV. Smoking-induced diffuse interstitial lung diseases. Thorax 2007;62(10):904–910.
69. Holt RM, Schmidt RA, Godwin JD, Raghu G. High resolution CT in respiratory bronchiolitis-associated interstitial lung disease. J Comput Assist Tomogr 1993;17(1):46–50.
70. MacRedmond R, Logan PM, Lee M, Kenny D, Foley C, Costello RW. Screening for lung cancer using low dose CT scanning. Thorax 2004;59(3):237–241.

71. Sverzellati N, Guerci L, Randi G, et al. Interstitial lung diseases in a lung cancer screening trial. Eur Respir J 2011;38(2):392–400.
72. Washko GR, Hunninghake GM, Fernandez IE, et al. Lung volumes and emphysema in smokers with interstitial lung abnormalities. N Engl J Med 2011;364(10):897–906.
73. Jin GY, Lynch D, Chawla A, et al. Interstitial lung abnormalities in a CT lung cancer screening population: prevalence and progression rate. Radiology 2013;268(2):563–571.
74. Verschakelen JA, Scheinbaum K, Bogaert J, Demedts M, Lacquet LL, Baert AL. Expiratory CT in cigarette smokers: correlation between areas of decreased lung attenuation, pulmonary function tests and smoking history. Eur Radiol 1998;8(8):1391–1399.
75. Katzenstein AL, Mukhopadhyay S, Zanardi C, Dexter E. Clinically occult interstitial fibrosis in smokers: classification and significance of a surprisingly common finding in lobectomy specimens. Hum Pathol 2010;41(3): 316–325.
76. Kawabata Y, Hoshi E, Murai K, et al. Smoking-related changes in the background lung of specimens resected for lung cancer: a semiquantitative study with correlation to postoperative course. Histopathology 2008;53(6): 707–714.
77. Remy-Jardin M, Edme JL, Boulenguez C, Remy J, Mastora I, Sobaszek A. Longitudinal follow-up study of smoker's lung with thin-section CT in correlation with pulmonary function tests. Radiology 2002;222(1):261–270.
78. Portnoy J, Veraldi KL, Schwarz MI, et al. Respiratory bronchiolitis-interstitial lung disease: long-term outcome. Chest 2007;131(3):664–671.
79. Nakanishi M, Demura Y, Mizuno S, et al. Changes in HRCT findings in patients with respiratory bronchiolitis-associated interstitial lung disease after smoking cessation. Eur Respir J 2007;29(3):453–461.
80. Heyneman LE, Ward S, Lynch DA, Remy-Jardin M, Johkoh T, Müller NL. Respiratory bronchiolitis, respiratory bronchiolitis-associated interstitial lung disease, and desquamative interstitial pneumonia: different entities or part of the spectrum of the same disease process? AJR Am J Roentgenol 1999;173(6):1617–1622.
81. Vassallo R, Jensen EA, Colby TV, et al. The overlap between respiratory bronchiolitis and desquamative interstitial pneumonia in pulmonary Langerhans cell histiocytosis: high-resolution CT, histologic, and functional correlations. Chest 2003;124(4):1199–1205.
82. Hartman TE, Primack SL, Swensen SJ, Hansell D, McGuinness G, Müller NL. Desquamative interstitial pneumonia: thin-section CT findings in 22 patients. Radiology 1993;187(3):787–790.
83. Koyama M, Johkoh T, Honda O, et al. Chronic cystic lung disease: diagnostic accuracy of high-resolution CT in 92 patients. AJR Am J Roentgenol 2003;180(3):827–835.
84. Akira M, Yamamoto S, Hara H, Sakatani M, Ueda E. Serial computed tomographic evaluation in desquamative interstitial pneumonia. Thorax 1997;52(4):333–337.
85. Kawabata Y, Takemura T, Hebisawa A, et al. Desquamative interstitial pneumonia may progress to lung fibrosis as characterized radiologically. Respirology 2012;17(8): 1214–1221.
86. Müller NL, Staples CA, Miller RR. Bronchiolitis obliterans organizing pneumonia: CT features in 14 patients. AJR Am J Roentgenol 1990;154(5):983–987.
87. Lee KS, Kullnig P, Hartman TE, Müller NL. Cryptogenic organizing pneumonia: CT findings in 43 patients. AJR Am J Roentgenol 1994;162(3):543–546.
88. Lee JS, Lynch DA, Sharma S, Brown KK, Müller NL. Organizing pneumonia: prognostic implication of high-resolution computed tomography features. J Comput Assist Tomogr 2003;27(2):260–265.
89. Lee JW, Lee KS, Lee HY, et al. Cryptogenic organizing pneumonia: serial high-resolution CT findings in 22 patients. AJR Am J Roentgenol 2010;195(4):916–922.
90. Ujita M, Renzoni EA, Veeraraghavan S, Wells AU, Hansell DM. Organizing pneumonia: perilobular pattern at thin-section CT. Radiology 2004;232(3):757–761.
91. Kim SJ, Lee KS, Ryu YH, et al. Reversed halo sign on high-resolution CT of cryptogenic organizing pneumonia: diagnostic implications. AJR Am J Roentgenol 2003;180(5):1251–1254.
92. Roberton BJ, Hansell DM. Organizing pneumonia: a kaleidoscope of concepts and morphologies. Eur Radiol 2011;21(11):2244–2254.
93. Flowers JR, Clunie G, Burke M, Constant O. Bronchiolitis obliterans organizing pneumonia: the clinical and radiological features of seven cases and a review of the literature. Clin Radiol 1992;45(6):371–377.
94. Maldonado F, Daniels CE, Hoffman EA, Yi ES, Ryu JH. Focal organizing pneumonia on surgical lung biopsy: causes, clinicoradiologic features, and outcomes. Chest 2007;132(5):1579–1583.
95. Akira M, Yamamoto S, Sakatani M. Bronchiolitis obliterans organizing pneumonia manifesting as multiple large nodules or masses. AJR Am J Roentgenol 1998;170(2):291–295.
96. Domingo JA, Pérez-Calvo JI, Carretero JA, Ferrando J, Cay A, Civeira F. Bronchiolitis obliterans organizing pneumonia: an unusual cause of solitary pulmonary nodule. Chest 1993;103(5):1621–1623.
97. Haddock JA, Hansell DM. The radiology and terminology of cryptogenic organizing pneumonia. Br J Radiol 1992;65(776):674–680.
98. King TE Jr. BOOP: an important cause of migratory pulmonary infiltrates? Eur Respir J 1995;8(2):193–195.
99. Galvin JR, Frazier AA, Franks TJ. Collaborative radiologic and histopathologic assessment of fibrotic lung disease. Radiology 2010;255(3):692–706.
100. Jara-Palomares L, Gomez-Izquierdo L, Gonzalez-Vergara D, et al. Utility of high-resolution computed tomography and BAL in cryptogenic organizing pneumonia. Respir Med 2010;104(11):1706–1711.
101. Arakawa H, Kurihara Y, Niimi H, Nakajima Y, Johkoh T, Nakamura H. Bronchiolitis obliterans with organizing pneumonia versus chronic eosinophilic pneumonia: high-resolution CT findings in 81 patients. AJR Am J Roentgenol 2001;176(4):1053–1058.
102. Johkoh T, Müller NL, Taniguchi H, et al. Acute interstitial pneumonia: thin-section CT findings in 36 patients. Radiology 1999;211(3):859–863.
103. Primack SL, Hartman TE, Ikezoe J, Akira M, Sakatani M, Müller NL. Acute interstitial pneumonia: radiographic and CT findings in nine patients. Radiology 1993;188(3): 817–820.
104. Desai SR, Wells AU, Rubens MB, Evans TW, Hansell DM. Acute respiratory distress syndrome: CT abnormalities at long-term follow-up. Radiology 1999;210(1):29–35.
105. Ichikado K, Suga M, Müller NL, et al. Acute interstitial pneumonia: comparison of high-resolution computed tomography findings between survivors and nonsurvivors. Am J Respir Crit Care Med 2002;165(11):1551–1556.
106. Ichikado K, Suga M, Muranaka H, et al. Prediction of prognosis for acute respiratory distress syndrome with thin-section CT: validation in 44 cases. Radiology 2006;238(1): 321–329.
107. Tomiyama N, Müller NL, Johkoh T, et al. Acute respiratory distress syndrome and acute interstitial pneumonia: comparison of thin-section CT findings. J Comput Assist Tomogr 2001;25(1):28–33.
108. Mihara N, Johkoh T, Ichikado K, et al. Can acute interstitial pneumonia be differentiated from bronchiolitis obliterans organizing pneumonia by high-resolution CT? Radiat Med 2000;18(5):299–304.
109. Tomiyama N, Müller NL, Johkoh T, et al. Acute parenchymal lung disease in immunocompetent patients: diagnostic accuracy of high-resolution CT. AJR Am J Roentgenol 2000;174(6):1745–1750.
110. Daimon T, Johkoh T, Sumikawa H, et al. Acute eosinophilic pneumonia: thin-section CT findings in 29 patients. Eur J Radiol 2008;65(3):462–467.
111. Collard HR, Moore BB, Flaherty KR, et al. Acute exacerbations of idiopathic pulmonary fibrosis. Am J Respir Crit Care Med 2007;176(7):636–643.
112. Akira M, Kozuka T, Yamamoto S, Sakatani M. Computed tomography findings in acute exacerbation of idiopathic pulmonary fibrosis. Am J Respir Crit Care Med 2008;178(4):372–378.

113. Fujimoto K, Taniguchi H, Johkoh T, et al. Acute exacerbation of idiopathic pulmonary fibrosis: high-resolution CT scores predict mortality. Eur Radiol 2012;22(1):83–92.
114. Silva CI, Müller NL, Fujimoto K, et al. Acute exacerbation of chronic interstitial pneumonia: high-resolution computed tomography and pathologic findings. J Thorac Imaging 2007;22(3):221–229.
115. Park IN, Kim DS, Shim TS, et al. Acute exacerbation of interstitial pneumonia other than idiopathic pulmonary fibrosis. Chest 2007;132(1):214–220.
116. Johkoh T, Müller NL, Pickford HA, et al. Lymphocytic interstitial pneumonia: thin-section CT findings in 22 patients. Radiology 1999;212(2):567–572.
117. Honda O, Johkoh T, Ichikado K, et al. Differential diagnosis of lymphocytic interstitial pneumonia and malignant lymphoma on high-resolution CT. AJR Am J Roentgenol 1999;173(1):71–74.
118. Johkoh T, Ichikado K, Akira M, et al. Lymphocytic interstitial pneumonia: follow-up CT findings in 14 patients. J Thorac Imaging 2000;15(3):162–167.
119. Frankel SK, Cool CD, Lynch DA, Brown KK. Idiopathic pleuroparenchymal fibroelastosis: description of a novel clinicopathologic entity. Chest 2004;126(6): 2007–2013.
120. Reddy TL, Tominaga M, Hansell DM, et al. Pleuroparenchymal fibroelastosis: a spectrum of histopathological and imaging phenotypes. Eur Respir J 2012;40(2):377–385.
121. Piciucchi S, Tomassetti S, Casoni G, et al. High resolution CT and histological findings in idiopathic pleuroparenchymal fibroelastosis: features and differential diagnosis [letter]. Respir Res 2011;12(1):111. http://www.respiratory-research.com/content/12/1/111. Published August 23, 2011. Accessed February 1, 2015.
122. Ryerson CJ, Urbania TH, Richeldi L, et al. Prevalence and prognosis of unclassifiable interstitial lung disease. Eur Respir J 2013;42(3):750–757.

This journal-based SA-CME activity has been approved for ***AMA PRA Category 1 Credit™.*** *See www.rsna.org/education/search/RG.*